## PERSPECTIVE

Check for updates

# Layered 2D PtX$_2$ (X = S, Se, Te) for the electrocatalytic HER in comparison with Mo/WX$_2$ and Pt/C: are we missing the bigger picture?

Sengeni Anantharaj [ID] *[ab] and Suguru Noda [ID] [ab]

The hydrogen evolution reaction (HER) is best catalyzed by metallic Pt with the lowest overpotential, Tafel slope, and highest exchange current density. But its scarcity made us look for abundant alternatives which come at the price of poor activity and stability. Hence, all non-Pt HER electrocatalysts are compared with Pt (often Pt/C). In such cases, a closer activity to that of Pt is usually appreciated for non-Pt materials. In contrast, when an HER electrocatalyst is made of Pt, it is expected to surpass the activity of Pt/C as it has the same Pt. A familiar example of this kind is the dilution of Pt without any compromise in activity. The recently evolved layered dichalcogenides of Pt (PtX$_2$) do not satisfy this expectation as they not only perform poorer than Pt/C but also against other familiar MX$_2$ HER electrocatalysts such as MoX$_2$ and WX$_2$. However, the studies that engaged in the evaluation of the HER activity of PtX$_2$ were quite useful in deducing the structure–activity relationship and mechanism which are clearly inevitable pieces of knowledge needed in all kinds of electrocatalysis. Though PtX$_2$ are poorer HER catalysts in their pristine form, structural engineering and other activation methods made them as active as Pt/C while a few were better than Pt/C. This perspective is dedicated to presenting the recent progress in the area of the PtX$_2$ catalyzed HER in comparison with MoX$_2$ and WX$_2$ while highlighting the opportunities and challenges. Particularly, how we are missing the bigger picture in designing a Pt-based HER electrocatalyst and the ways in which poorly active PtX$_2$ can be made into a superior one to Pt/C are critically discussed.

[a] *Department of Applied Chemistry, School of Advanced Science and Engineering, Waseda University, 3-4-1 Okubo, Shinjuku-ku, Tokyo 169-8555, Japan.*
*E-mail: ananth@aoni.waseda.jp, anantharaj1402@gmail.com*
[b] *Waseda Research Institute for Science and Engineering, Waseda University, 3-4-1 Okubo, Shinjuku-ku, Tokyo 169-8555, Japan*
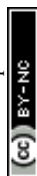
**Sengeni Anantharaj**

*Dr Sengeni Anantharaj obtained his PhD in 2018 from CSIR-CECRI, Karaikudi, Tamil Nadu, India, following which he worked with Prof. Noda as a JSPS postdoc fellow from January 2019 to March 2021. Currently, he is an Assistant Professor (Junior Researcher) at RISE, Waseda University since April 2021. He was the first 'ECS India Section S. K. Rangarajan Graduate Student Award' winner of the year 2017 which was presented to him by The Electrochemical Society, USA, for his noteworthy works in the area of electrocatalysis and materials electrochemistry during his PhD. He is an electrochemist by passion and a (teaching) researcher by profession. He places his interest on everything where there is a transfer of electrons that results in the transformation of matter, especially at the electrode–electrolyte interface.*

**Suguru Noda**

*Prof. Suguru Noda received his PhD in 1999 from The University of Tokyo, Japan, became an assistant professor and associate professor there, and then joined Waseda University in 2012 as a full professor. He is a chemical engineer conducting research in the field of materials processes. He has recently been focusing on the practical production of carbon and silicon nanomaterials such as carbon nanotubes and silicon films/nanoparticles, and applying these materials to energy and electronic devices including rechargeable batteries.*

This journal is © The Royal Society of Chemistry 2022

*Energy Environ. Sci.*, 2022, **15**, 1461–1478 | **1461**

**Broader context**

Energy conversion electrocatalysis ranging from water electrolysis and fuel cells to recently attention-grabbing $CO_2$ and $N_2$ electrolysis depends mainly on the development of highly efficient electrocatalysts in terms of activity, stability, and selectivity. In that context, it has always been a custom to compare all the newly developed catalysts with the state-of-the-art of the field. The same is also true for the electrocatalytic hydrogen evolution reaction (HER) where Pt is the state-of-the-art. The ultimate goals in the HER are no Pt, low-Pt, and better kinetics in a medium where Pt alone cannot perform better. The recent evolution of $PtX_2$ as HER electrocatalysts has concerned the community as they do not perform better than Pt/C despite the fact that they are also made of Pt. A material that takes a huge amount of time, energy, and resources to make but performs poorer than Pt is not as encouraging as the advancements being made with other HER electrocatalysts. Hence, it is essential to ensure that the developments happening in the field of HER electrocatalysis are focused on the ultimate goals and the bigger picture of the field rather than being driven by the fancy structural properties of a particular class of materials (*i.e.*, $PtX_2$).

# Introduction

The hydrogen evolution reaction (HER) is the cathodic half-cell reaction of water electrolysis that governs the $H_2$ generation efficiency significantly alongside the anodic oxygen evolution reaction (OER).[1–6] Though the kinetic complexity of the OER attracted significant attention earlier, the HER has also gained equal attention in recent years as the significance of replacing or lowering the amount of Pt used and improving the poor kinetics of Pt in the alkaline HER are realized.[7–14] In general, catalysts that have little or no Pt suffer from poor activity and kinetics in all media. On the other hand, Pt-based HER catalysts suffer from poor kinetics when the concentration of protons available in the solution is very low or nil (*i.e.*, in highly alkaline solutions).[8,10,15] In such cases, the proton adsorption and discharge step (Volmer step) is coupled with water dissociation. Recently, several advancements have been made to overcome this particular issue in the alkaline HER among which heterostructuring Pt with a metal hydroxide co-catalyst and doping Ru in limited proportions are the most efficient ones.[7,8,16] Materials that contain Pt and Ru are the only known HER electrocatalysts to have an onset potential of 0.0 V *vs.* RHE and demand low overpotentials under benchmarking conditions with a few exceptional metal phosphides of Fe and Co.[6] Promising alternatives to Pt are chalcogenides, phosphides, nitrides, and carbides of transition metals that include but are not limited to Ni, Co, Fe, Cu, Mn, W, Mo, Rh, and Re.[3,6,17] Particularly, phosphides of Fe and its alloys show very close HER activity to those of Pt and Pt-based HER electrocatalysts.[18–22] However, it is difficult to prepare phosphides, carbides, and nitrides and they always require high pressure and temperature conditions with an inert atmosphere.[14,23–26] On the other hand, chalcogenides have always been obtained under relatively milder conditions and often show appreciable HER activity in terms of an overpotential at 10 mA cm$^{-2}$ (apparent activity) that is just 50 to 80 mV higher than that of metal phosphides and 80 to 150 mV higher than those of Pt and Ru-based catalysts.[1,9,27] Chalcogenides of first-row transition metals (mainly of Ni, Co, Fe, and Cu) are of different stoichiometries and catalyze the HER distinctly depending on the metal to chalcogen ratio.[3,28] However, these metals rarely form 2D layered structures as their electronic configurations are usually not fit for the formation of octahedral and trigonal prismatic phases. Layered 2D transition metal chalcogenides (TMDs), on the other hand, are the most preferred form of crystallization for many transition metal cations in their tetravalent state including W, Mo, and Pt. These materials are of recent interest in the area of energy conversion electrocatalysis because of their fascinating physical and chemical properties and their structural resemblance to graphene.[29–32] Among them, $WX_2$ and $MoX_2$ are reported in vast counts in the literature for their synthesis, and optical, electronic, spintronic, magnetic, and electrocatalytic properties.[33–38] Tetravalent cations of both Mo and W have just two electrons in their d-orbitals which tend to degenerate in a trigonal prismatic fashion and always result in a semiconducting 2H phase under ordinary synthetic conditions.[29] On the other hand, the tetravalent cation of Pt having six d-electrons degenerates into octahedral symmetry in which the $t_{2g}$ level can be completely filled. Hence, $PtX_2$ always and almost crystallizes in the metallic 1T phase.[33,39] TMDs of W, Mo, and Pt have been reported for the HER recently in literature more often now than ever mainly because of the recent revolution in the area of materials science and technology. $MoX_2$ and $WX_2$ are certainly worth reporting for the HER as they possess better activity than metallic Mo and W.[40–42] In contrast, pristine $PtX_2$ can never perform better than its metallic counterpart Pt in HER electrocatalysis.[39] In that context, it is meaningless to toil with $PtX_2$ just to have a poorer HER electrocatalyst when we actually have the state-of-the-art metallic Pt. However, other advancements (*i.e.*, recent understanding of how $PtX_2$ works in HER electrocatalysis in comparison with other $MX_2$ materials and the use of $PtX_2$ as a good starting material or a pre-catalyst for making an excellent HER electrocatalyst) made in this area are worthy of a critical discussion. Thus, this can lead to further advancements in the area of HER electrocatalysis and associated catalyst design strategies. This perspective comes with such a critical opinionated discussion on the recent developments in the area of $PtX_2$ design and application to HER electrocatalysis.

# TMDs: an overview

TMDs are a unique class of materials formed by transition metals when they combine chemically with the chalcogenide

**1462** | *Energy Environ. Sci.*, 2022, **15**, 1461–1478

This journal is © The Royal Society of Chemistry 2022

anions with a general formula of $MX_2$ in which M is a tetravalent transition metal cation and X is a chalcogenide dianion.[38] Any transition metal that can have an electronically stable 4+ oxidation state can form TMDs. TMDs resemble 2D graphene in their structure and tend to have resonating properties.[30,39,43–49] Very common transition metals with a stable 4+ oxidation state and a capability of forming TMDs are W, Mo, Ti, Cr, Mn, Re, Pd, and Pt. Among them, TMDs of Mo and W are the most frequently used HER electrocatalysts. TMDs formed by these stable tetravalent cations of transition metals commonly crystallize in trigonal prismatic (2H) and octahedral (1T) lattices (Fig. 1a and b) of which the 2H-phase is semiconducting and the 1T-phase is metallic. Other than these two phases, a few $M^{4+}$ ions from the transition metal series are known to form the semiconducting 3R phase of the same trigonal prismatic lattice system to that of the 2H phase but with a different point of symmetry under non-standard conditions.[50] In recent years, the relationship between the d-electron population and the degeneracy of electronic states upon forming TMDs is correlated. Tetravalent transition metal cations with incompletely filled d-orbitals (e.g. $W^{4+}$ and $Mo^{4+}$ with four d-electrons) degenerate into e′ ($d_{xz,yz}$), $a_1$ ($d_{z^2}$), and e ($d_{x^2-y^2,xy}$) sub-levels forming the trigonal prismatic structure so as to have a high crystal field stabilization. On the other hand, tetravalent cations with more than four d-electrons degenerate into $e_g$ ($d_{z^2,x^2-y^2}$) and $t_{2g}$ ($d_{xy,yz,xz}$) sub-levels forming the octahedral structure.[30] A familiar example of this kind is $Pt^{4+}$ with six d-electrons.[39]

When $Pt^{4+}$ undergoes electronic degeneration to result in an octahedral geometry, the $t_{2g}$ sub-level gets completely filled

which in turn results in high crystal field stabilization. Between the 2H and 1T phases of TMDs, the latter was found to be outperforming the former as it is metallic in nature, thus, offers a better charge transfer during the HER. On the other hand, the 2H phase of $MoX_2$ and $WX_2$ in a few cases was found to transform into the 1T phase during the HER as $Mo^{4+}$ and $W^{4+}$ cations are reduced electrochemically in the potential window of the HER.[49,51] However, it is not shown that such a transformation is possible with other $MX_2$ catalysts under similar conditions. As far as the synthesis is concerned, high-quality oxygen impurity-free TMDs are obtained only *via* physical methods in a vacuum. Vapor deposition, sputtering, and laser ablation are the ones prominently used in this area.[52–54] Though aqueous routes are known to impart a considerable quantity of oxygen impurities, their effect on HER activity is poorly understood. Hence, irrespective of the method by which the TMDs are synthesized and the lattice system in which they crystallized into, their HER activity tends not to vary much unless other modes of material engineering strategies are deployed to enhance the activities additionally. The most common material engineering strategies used with TMDs are amorphization, making defects and vacancies, and chemically opening up the basal planes by rupturing M–X bonds and creating more edges.[41,55–57] Other than these, compositing, heterostructuring, anion exchange, and doping have also been shown to enhance the HER activity of these TMDs as these strategies are known to bring out HER-favouring changes in their electronic structures.[58–61] The electronic structure of a catalyst is crucial in HER electrocatalysis as it reveals the density of states (DOS) at different applied potentials. In general, materials with a significant DOS intensity at and around 0 eV are better for the HER as the reversible potential of HER is 0.0 V *vs.* RHE. Having a high DOS intensity at 0.0 eV ensures a better charge transfer at and around the reversible potential of the HER which is the most important requirement of all for an electrocatalyst.[62]

Unlike many other energy conversion electrocatalytic reactions, the HER does not require the catalytic site to undergo a self-redox cycle to catalyse the evolution of $H_2$. All that happens in the HER is adsorption of proton (water dissociation coupled-proton adsorption in alkali), discharge, and delivery of $H_2$ and hence, the DOS matters the most besides the energy of interactions of proton/water and M–H intermediates. Fig. 2 shows the electronic structure of a few commonly used TMDs for the HER in comparison with Pt and $PtO_2$.[63] Among them, Pt is the better HER electrocatalyst than all and the same is witnessed by its electronic structure and high DOS intensity at 0.0 eV. For materials with a weak and too strong proton/water adsorption free energy change, the overpotential (work required to evolve $H_2$) is considerably higher. Such materials, even when supported by HER-favouring DOS intensities will perform poorly because of their opposing energy of interaction with reaction intermediates. Familiar examples for this kind are Ru and Ni, these two metals have HER-favouring DOS intensities at and around 0.0 eV but they form strong metal hydride bonds prohibiting the easier delivery of $H_2$. Particularly, Ru has the
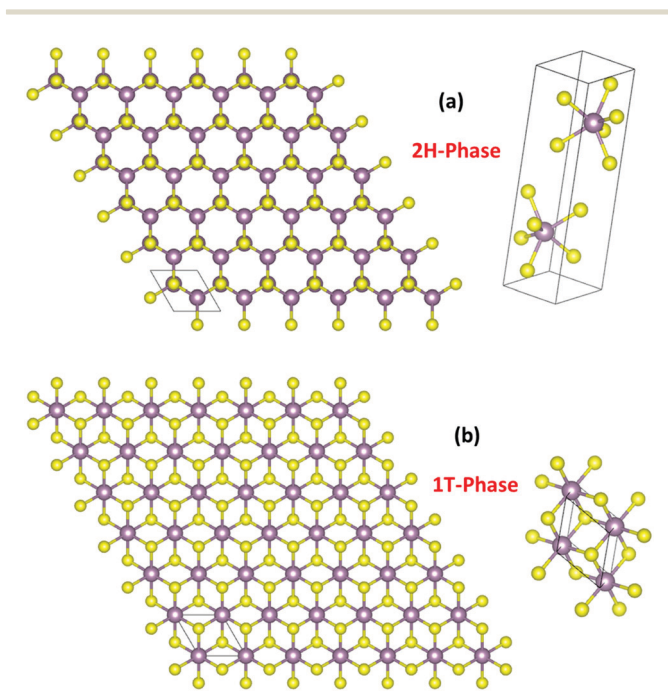


Fig. 1 2H (a) and 1T (b) phases formed commonly by TMDs with the unit cells showing trigonal prismatic and octahedral arrangements of atoms, respectively.
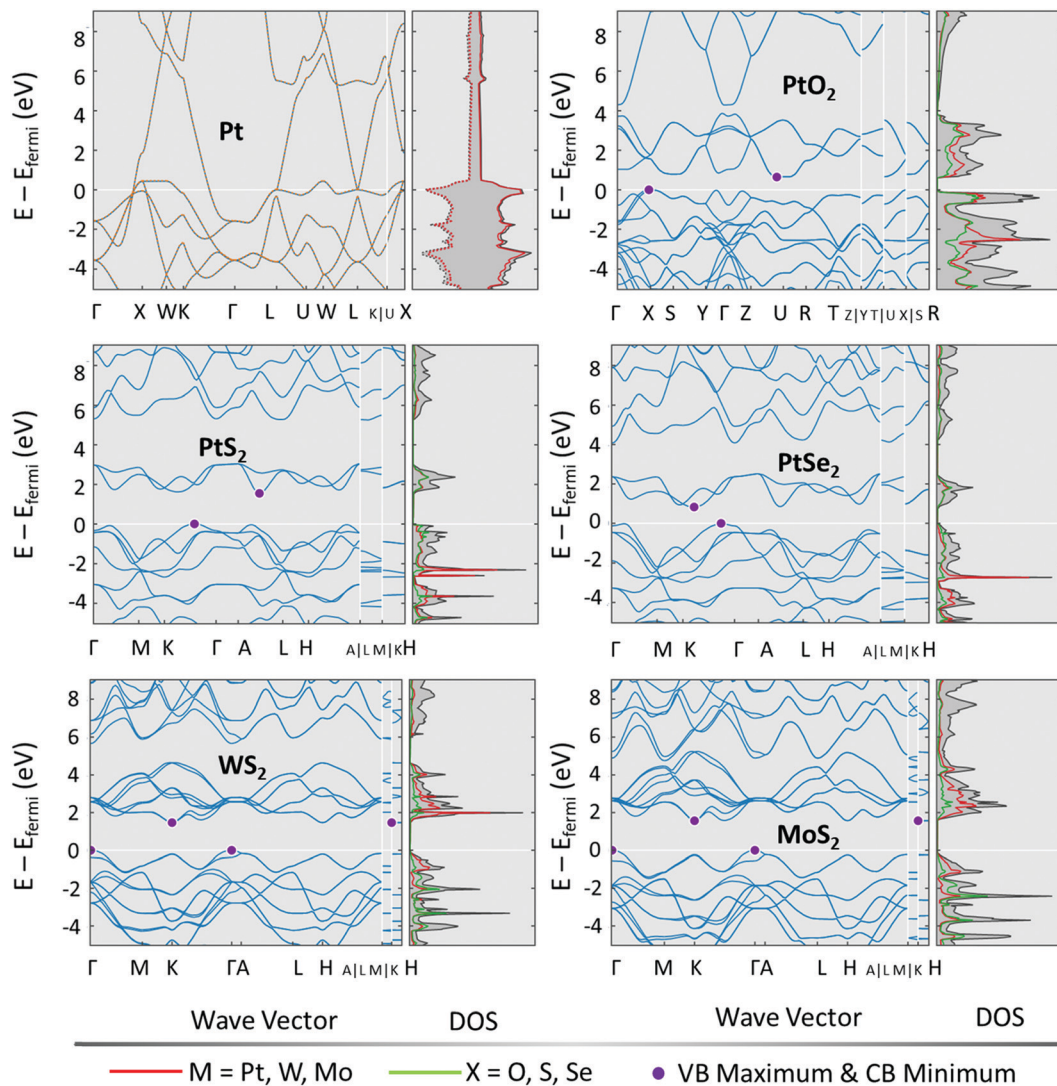
This journal is © The Royal Society of Chemistry 2022

*Energy Environ. Sci.*, 2022, **15**, 1461–1478 | **1463**

**Fig. 2** Electronic band structures with DOS for Pt, $PtO_2$, $PtS_2$, $PtSe_2$, $WS_2$, and $MoS_2$. Reproduced with permission from ref. 64 copyright (2012, materials project).

same onset as that of Pt because of their similar DOS maps yet the exchange current density of Ru remains a few orders lower than that of Pt because of its nature of forming strong hydride bonds.[7,64] Hence, for designing an efficient HER electrocatalyst, it is essential to pay attention to both the electronic structure and the energies of the interaction of intermediates involved.

## Things to go after in the HER

The HER is the cathodic half-cell reaction of water electrolysis which is relatively simpler than its counterpart, the anodic OER in terms of mechanism. Even though the OER is the one that takes up a huge amount of energy due to its sluggish kinetics, understanding the mechanism of the HER is also inevitable in order to design an efficient electrocatalyst. There are only two elementary steps in the HER, namely, adsorption of

proton/water and subsequent discharge (*i.e.*, the Volmer step: $H^+/H_2O + e^- + S \rightarrow S–H$ (+$OH^-$) that results in a hydridic intermediate (S–H)) and the evolution of $H_2$ either by repeating the Volmer step *via* the hydridic intermediate (*i.e.*, the Heyrovsky step: $S–H + H^+/H_2O + e^- \rightarrow H_2 \uparrow + S$(+$OH^-$)) or *via* chemical release of $H_2$ from two adjacent hydridic intermediates (*i.e.*, the Tafel step: $2S–H \rightarrow 2S + H_2\uparrow$). In theory, the HER is the reaction that occurs at 0.0 V *vs.* RHE on the surface of a standard hydrogen electrode ($Pt(s)|1$ M $[H^+]/H_{2(g)}$ 1 atm) at pH 0 and against RHE under all conditions.[5] There are only two other elements (Ru and Rh) which can have an onset potential of 0.0 V *vs.* RHE for the HER.[7,65] However, their exchange current density is too low when compared to that of Pt because of their strong adsorption tendency towards H and OH adatoms that result during the HER. Hence, Pt is still the best of all.[64] However, there have been notable developments in recent years in the area of catalyst design. In the last five years, many non-Pt catalysts have been reported to have excellent HER activity in

both acid and alkali and there are several reviews on the same.[6,9] Hence, further research and development in this area of energy conversion have recently attracted greater attention.

As for every electrocatalyst, HER electrocatalysts are also screened for their activity, stability, and selectivity.[66] In extreme pH conditions, there is neither a catalyst-confined self-redox reaction nor an electrolyte-based competing reaction. Hence, selectivity is not an issue with most of the HER electrocatalysts. Stability, on the other hand, is tested by both potentiodynamic sweeping techniques and controlled current/potential voltammetry and for most of the metal-based HER electrocatalysts, it is quite good. However, the stability of most of the alkaline HER electrocatalysts is poorer where the water dissociation coupled Volmer step (proton adsorption and discharge) and highly alkaline environment cause anion exchange at the surface leading to the formation of metal hydroxide containing heterostructures.[8,67] It has recently been understood that a metal hydroxide interface is essential to realize better HER activity in alkaline medium even with Pt and Ru which are known for their exceptionally lower overpotentials at benchmarking conditions.[7] As stability and selectivity are almost of no concern in the HER, activity is given greater attention. In general, the activity of any electrocatalyst can be classified into apparent activity and intrinsic activity in which the former is the performance of the catalyst in practical conditions while the latter is the true activity of the catalyst free from the effects of iR drop, surface area, and mass.[68,69] The intrinsic activity forms the base for further optimization and structural engineering to realize a better apparent activity under practical conditions. The apparent activity of an HER electrocatalyst is given by the overpotential at a fixed current density which is usually 10 mA cm$^{-2}$, exchange current density, and mass activity whereas intrinsic activity is given only by turnover frequency (TOF) and specific activity at a given overpotential. Both the TOF and specific activity require the knowledge of the real surface area, the exact number of active sites, and faradaic efficiency (FE) for precise determination.[69] Between the TOF and specific activity, the former is a straightforward measure of the intrinsic activity of an electrocatalyst. We have detailed the ways in which all these activity markers can be precisely obtained in our earlier reviews and perspectives.[66,68] In addition to these three primary evaluation parameters (activity, selectivity, and stability), mechanistic evaluation by Tafel analysis is also inevitable. In HER electrocatalysis, Tafel analysis provides vital information on the mechanism and relative information on the kinetics. However, the use of potentiodynamic polarization curves for Tafel analysis has significantly led to the unintended falsification of data in the literature. To get precise values of the Tafel slope and exchange current density, it is strongly advised to use steady-state responses that are corrected for 100% iR drop. More detailed discussion on the appropriate ways of Tafel analysis can be found in our recent viewpoint article.[70] In general, a better HER electrocatalyst is anticipated to have lower overpotentials and higher TOF, exchange current density, stability, and selectivity.

# HER activity trends in PtX$_2$

Layered dichalcogenides of Pt$^{4+}$ ions with a d$^6$ electronic configuration always and almost prefer to degenerate into octahedral symmetry (i.e., 1T phase) unlike W$^{4+}$ and Mo$^{4+}$ ions. This 1T phase of TMDs is metallic and electronically highly conductive. Hence, it is obvious to anticipate that PtX$_2$ will perform better than MoX$_2$ and WX$_2$ for the HER. However, in practice, no such superior activity to that of MoX$_2$ and WX$_2$ is generally witnessed with PtX$_2$ especially when the latter is in its pristine form. Instead, most of the time, the activity reported for PtX$_2$ is only as good as those reported for MoX$_2$ and WX$_2$. However, there are exceptions where PtX$_2$ was shown to have better HER activity. In such exceptional cases, other factors (to be discussed in the latter part) have contributed more to the overall activity enhancement than the intrinsic activity of pristine PtX$_2$.

# PtX$_2$ with poorer HER activity than Pt or Pt/C

A general theoretical account on the HER activity of diselenide and disulphide of Pt was first given by Tsai and co-workers[71] along with a bunch of other metals including W and Mo. In this study, both 1T and 2H phases with basal plane termination and edge-site termination were examined. Since Pt$^{4+}$ ion can only form the 1T phase, for PtS$_2$ and PtSe$_2$, calculations were done only on the basal plane terminated and edge-terminated 1T phase. The Gibbs free energy changes associated with H-adsorption on the chalcogen site ($\Delta_{HX}$) and on Pt ($\Delta_H$) of PtS$_2$ and PtSe$_2$ are as follows. For the basal plane, $\Delta_H$ values are 1.35 and 1.44 eV, respectively. For the edge-site, the values (of $\Delta_H$) are $-0.08$ and $-0.02$ eV, respectively. For H-adsorption on the X site ($\Delta_{HX}$), the basal plane of PtS$_2$ and PtSe$_2$ showed 0.34 and $-0.18$ eV, respectively, whereas for the edge-site, both of them showed significantly higher negative values ($-0.84$ and $-0.93$ eV, respectively). These values are plotted against one another in Fig. 3a and b along with the values of other TMDs. In general, for a material to be more active in any electrocatalytic reaction, the Gibbs free energy change associated with the adsorption of an intermediate should be moderate. For the HER, the values should be closer to 0.0 eV in theory. A very high positive value for H-adsorption implies poor H-adsorption while a very high negative value implies spontaneous adsorption and the formation of a strong M–H bond. Both would require more energy to release the adsorbed H atoms as H$_2$ molecules. From the values provided above, it is explicit that only undercoordinated Pt atoms at the edge-site are appreciably active for the HER while the same Pt site in the basal plane and X sites in both the basal plane and edge-site are either too weak or too strong for H-adsorption. This information right away implies that PtX$_2$ cannot be as efficient as Pt or Pt/C for the HER. The same trend was supported by the simulated DOSs of PtS$_2$ and PtSe$_2$ (Fig. 3c) which when compared with the DOSs of other TMDs studied together in this report were found to be

This journal is © The Royal Society of Chemistry 2022
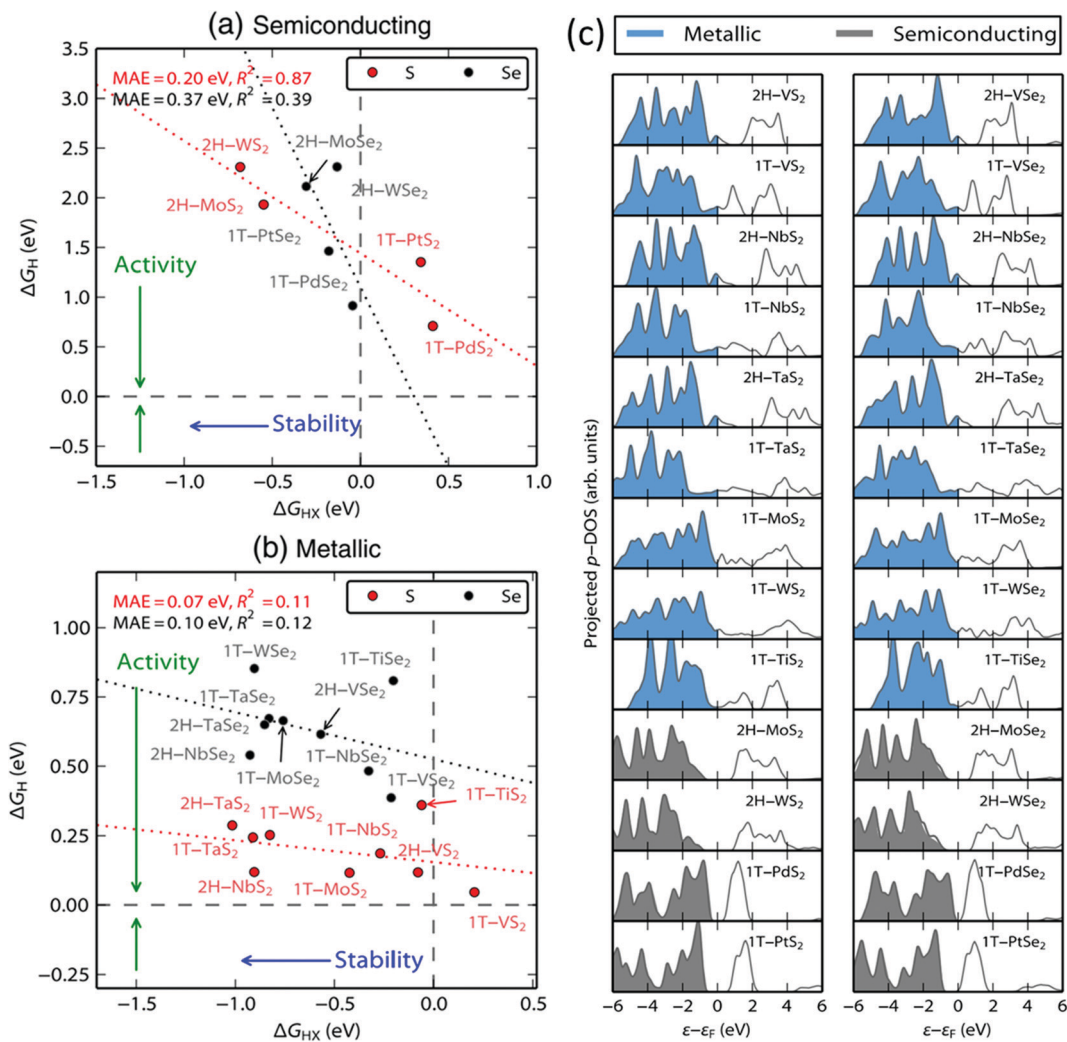
Energy Environ. Sci., 2022, 15, 1461–1478 | 1465

**Fig. 3**　(a and b) Plots of Gibbs free energy of H-adsorption on the metal site ($\Delta_H$) and on the chalcogen site ($\Delta_{HX}$) for various TMDs including W, Mo, and Pt for the semiconducting 2H phase and metallic 1T phase. (c) Projected DOS of various TMDs in comparison with that of W, Mo, and Pt showing no significant electron population for $PtS_2$ and $PtSe_2$ at around 0.0 eV. Reproduced with permission from ref. 71 (Copyright 2015, Elsevier).

having similar patterns and no population of electrons at around 0.0 eV. Soon after this study, Chia and co-workers[39] reported the monotonic dependence of HER activity of $PtX_2$ on the size of the chalcogen present in it. They found that the increasing size of the chalcogen increases the metallicity of $PtX_2$ as one goes from S to Te in the chalcogen group.
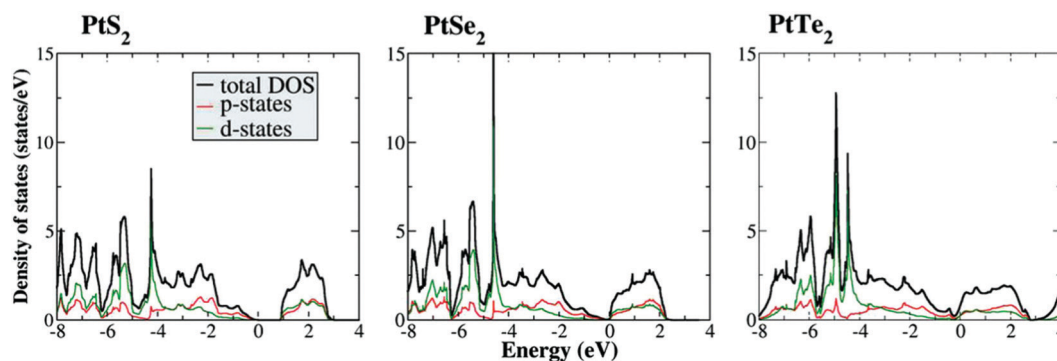


**Fig. 4**　Calculated DOSs of the p and d-states of $PtX_2$ (X = S, Se, and Te) showing an increasing metallic character and improved electron population at 0.0 eV with the increasing size of the chalcogen. Reproduced with permission from ref. 39 (Copyright 2016, Wiley).

Interestingly, the experimental results also resonated with their theoretical predictions (Fig. 4). However, none of this dichalcogenide was able to perform HER effectively when compared to Pt/C. This raises the question 'is it really meaningful to apply $PtX_2$ for the HER when we have a better performing catalyst of the same element (*i.e.*, Pt in the form of Pt/C)?'. Similar calculations but with significant changes in simulation parameters reported by Mir and co-workers,[72] Liu and co-workers,[73] and Huang and co-workers[74] have all concluded that $PtX_2$ can never catalyse the HER as efficiently as Pt/C. Very recently, Ma and Shen[75] also reported a similar trend even with vacancy engineering and Pd doping. Apart from these studies, there have been many experimental works as well. Particularly, the number of reports on $PtSe_2$ is higher despite it being shown to be poorer than $PtTe_2$. Lin and co-workers[76] reported the magnetron sputtering-assisted selenization of the Pt film to form $PtSe_2$ which showed poorer HER activity than Pt under identical conditions (Fig. 5a). Specifically, $PtSe_2$ delivered $-225$ mA cm$^{-2}$ at $-0.8$ V *vs.* RHE whereas Pt delivered $-510$ mA cm$^{-2}$ at the same potential.

Zhang and co-workers[77] have recently reported a two-step approach to grow edge-rich $PtSe_2$ on carbon cloth (CC) substrate in which Pt sputtering follows the selenization in an inert atmosphere at high temperature (Fig. 5b). When the thickness of the $PtSe_2$ film was varied as 10.7, 24.8, 51.1, and 100.2 nm (labelled as $PtSe_2$@CC-1, $PtSe_2$@CC-2, $PtSe_2$@CC-3, and $PtSe_2$@CC-4 in Fig. 5b), the HER activity was found to increase with the increasing thickness until 51.1 nm and began lowering afterward. Notably, none of these $PtSe_2$ films matched the activity of Pt under identical conditions. When both $PtX_2$ and Pt/C have the same precious metal (*i.e.*, Pt), preparing and applying $PtX_2$ for the HER appear to be meaningless as no $PtX_2$ can have a better HER activity than Pt/C.

However, valuable insights brought out by these studies on the role of layer numbers, the importance of having an edge-rich surface, the role of vacancies and defects, and the film thickness are something that deserves to be appreciated as these results are invaluable in understanding the patterns and trends of HER activity for a variety of TMDs. $PtTe_2$, on the other hand, is relatively less frequently reported in the literature though it was shown to be the best of $PtX_2$ for the HER earlier by Chia and co-workers.[39] Also, $PtTe_2$ is mostly reported with one or more additional metals. When there are additional metal sites, telluride of Pt has always and almost outperformed Pt/C. Classic examples of this kind are PtPdRuTe reported by Liu and co-workers[78] and the Pt/$PtTe_2$/NiCoTe$_2$ heterostructure reported by Yi and co-workers.[79] Similarly, $PtS_2$/TiC reported by Jeong and co-workers[80] and $PtSe_2$/Pt reported by Wang and co-workers[81] have performed as have done by Pt/C. Otherwise, none of the reported $PtX_2$ were able to surpass the activity exerted by Pt or Pt/C in the HER.

## Role of layer numbers and defects/vacancies on the HER activity of $PtX_2$

As introduced above, when there are one or more metals besides Pt in a $PtX_2$, the observed HER activity is always better than Pt or Pt/C. However, there are instances when such high HER activity was realized just with $PtX_2$. In such cases, increasing the number of layers of $PtX_2$ and creating defects/vacancies that would lead to the formation of metallic Pt clusters are behind this high HER activity. In general, $WX_2$ and $MoX_2$ are shown to exhibit enhancement in HER activity when the layer number is decreased by exfoliation as it leads to an increased active surface area. Hence, there have been many attempts of making and studying monolayers of $MoX_2$ and $WX_2$ to understand the origin of their HER activity.[82–85] The results have unanimously supported the fact that creation of more edges was the reason for enhanced HER electrocatalysis with $MoX_2$ and $WX_2$.[86–90] In sharp contrast to this trend, $PtX_2$ have shown decreasing activity with the decreasing layer numbers despite the fact that it also belongs to the family of isostructural layered 2D TMDs. This was quite intriguing and led to a few notable and dedicated works that studied the effect of layer numbers of $PtX_2$ and related electronic properties.
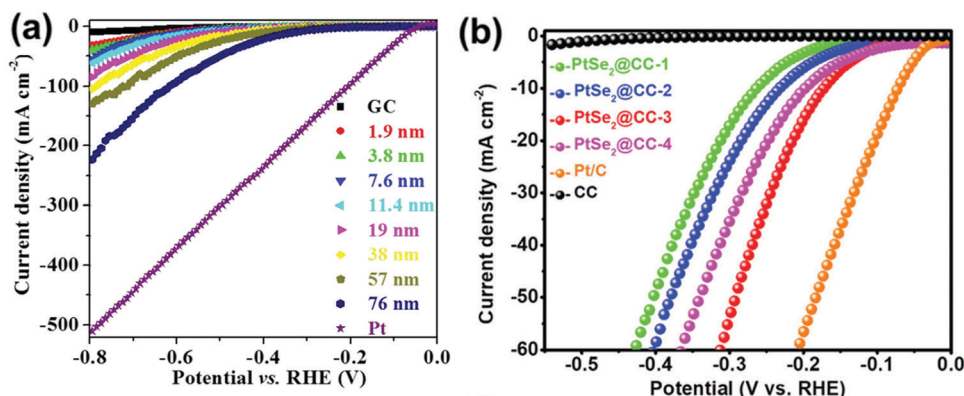


Fig. 5 (a) $PtSe_2$ with increasing HER activity with the increasing thickness. Reproduced from ref. 76 (Copyright 2017, Elsevier). (b) $PtSe_2$ thin films with the increasing HER activity with thickness until it reached 51.1 nm ($PtSe_2$@CC-3) and activity reversal thereafter. Reproduced with permission from ref. 77 (Copyright 2021, Royal Society of Chemistry). Notably, none of these films showed any comparable activity to that of Pt or Pt/C under identical conditions.
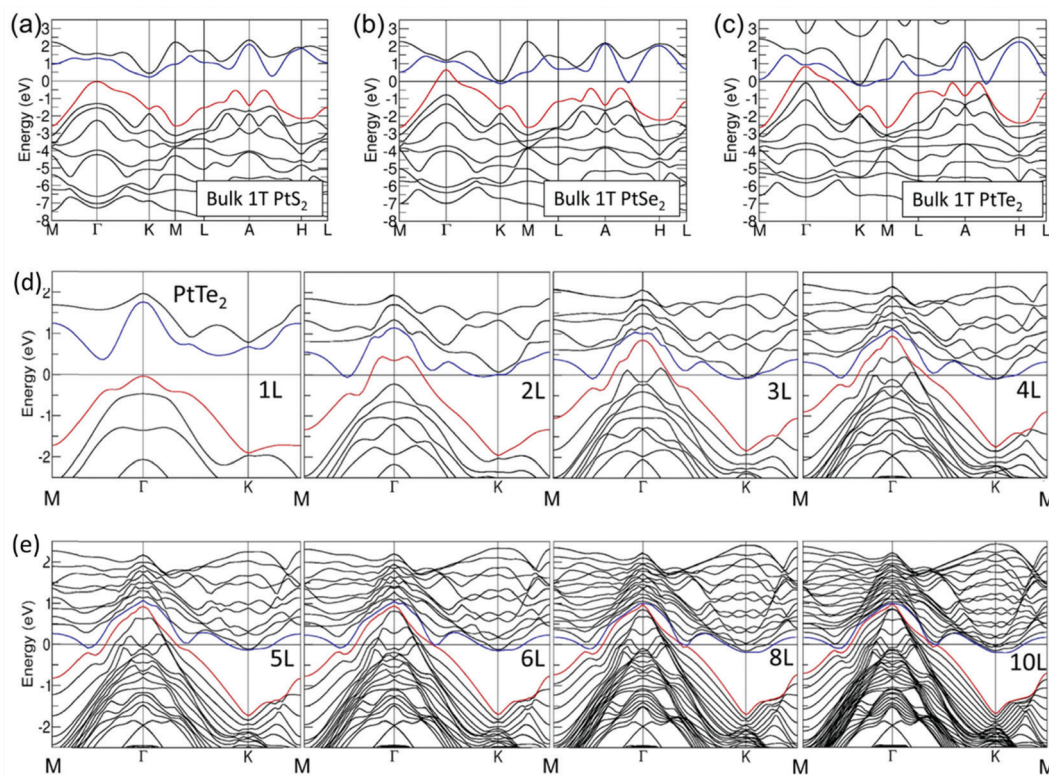
This journal is © The Royal Society of Chemistry 2022

*Energy Environ. Sci.*, 2022, **15**, 1461–1478 | **1467**

**Fig. 6** Electronic band structures of bulk 1T PtS$_2$ (a), bulk 1T PtSe$_2$ (b), and 1T PtTe$_2$ (c) with the electronic band structures of 1T PtTe$_2$ of 1–4 layers (d) and 5, 6, 8, and 10 layers (e) showing increasing metallicity and the overlap of conduction and valence bands with increasing layer numbers. Reproduced with permission from ref. 91 (Copyright 2019, Nature).

Villaos and co-workers[91] provided the theoretically calculated band structures for the 1T phase of bulk PtX$_2$ in comparison with the band structures of the same with increasing layer numbers from 1L to 10L of which the band structures of bulk 1T phases of PtS$_2$, PtSe$_2$, and PtTe$_2$ are shown together with the band structures of 1T PtTe$_2$ of layer numbers 1 to 10 in Fig. 6a–e. Evidently, the bulk phases of PtX$_2$ are more metallic in nature and the metallicity increases with the increasing size of the chalcogen as shown by Chia and co-workers[39] as well. The crossover of Fermi level over 0.0 eV was witnessed with the bulk 1T phases of PtSe$_2$ and PtTe$_2$ but not with PtS$_2$. This implies that no matter how many layers PtS$_2$ has, it will continue to have poor electronic conductivity which also accounts for its poor HER performance. Increasing layer numbers, on the other hand, showed the same trend for all three of them. Particularly, the crossover of the Fermi level over 0.0 eV was witnessed when there were four or more layers with PtSe$_2$ whereas for PtTe$_2$ this crossover was witnessed right away with the addition of the second layer (2L) which continues to increase with the increasing layers. In addition to that, clear overlaps of the conduction band and valence band were also witnessed with the increasing number of layers in PtTe$_2$. This increasing metallicity is the main reason why PtX$_2$ have an opposite activity trend to that of WX$_2$ and MoX$_2$ with the increasing number of layers. In the meantime, Hu and co-workers[92] have shown that with the increasing number of layers of 1T PtSe$_2$, HER activity increases

and edged closer to Pt/C when there were 20 layers (Fig. 7a–h). This observation aligns well with the predictions made by Villaos and co-workers and it was once again proven that PtX$_2$ is not like WX$_2$ or MoX$_2$ when it comes to the electrocatalytic HER. Even though the edge-sites remain to be the active sites with PtX$_2$ just like in WX$_2$ and MoX$_2$, increasing metallicity with the increasing layer numbers makes it behave entirely differently. With the increasing metallicity, the Pt-like character of PtX$_2$ does also increase leading to enhanced HER activity. This once again urges us to ask 'is it really meaningful to apply PtX$_2$ for the HER when it is clear that Pt or Pt/C is better in every aspect?'.

Defects or vacancies, in contrast, were sometimes found to bring out parallel activity to that of Pt/C. However, the origin of this high HER activity was not the PtX$_2$ sheets (basal plane or edge-site) but the undercoordinated Pt atoms and Pt clusters that were formed as a result of inducing defects and vacancies. These undercoordinated Pt atoms and Pt clusters are much like Pt or Pt/C in HER activity. Li and co-workers[93] have recently shown how creating ordered Te vacancies in PtTe$_2$ could make it perform better in the HER than Pt/C (Fig. 8a–f). To induce such ordered vacancies, they used the two-step top-down approach in which exfoliation followed the heat treatment.

The one with ordered single atom Te vacancies created by heating at 600 °C after exfoliation performed better than Pt/C. Detailed XPS and XANES investigations suggested that PtTe$_2$
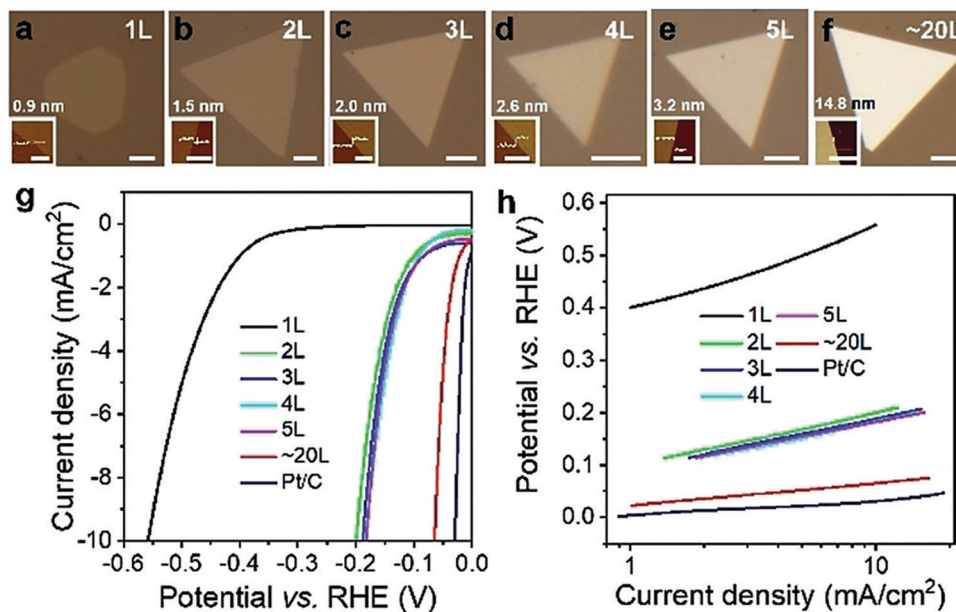
Fig. 7 (a–f) Optical images of PtSe$_2$ flakes grown using a chemical vapor transfer technique. (g and h) The corresponding HER LSVs and Tafel lines, respectively, showing better HER activity with the increasing number of layers. Reproduced with permission from ref. 92 (Copyright 2019, Wiley).
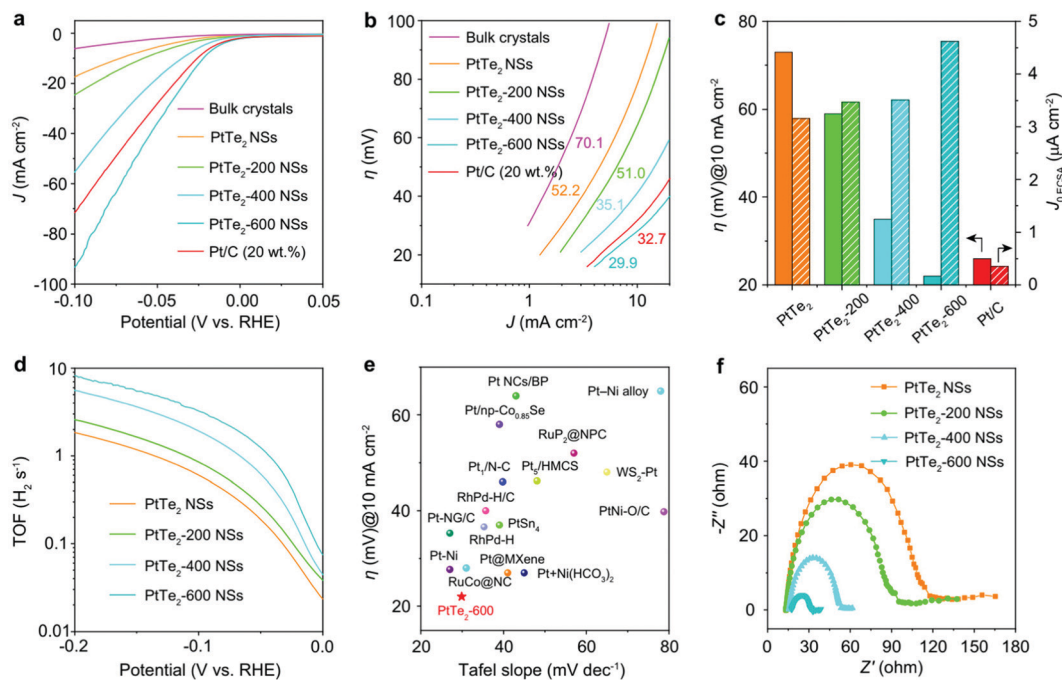


Fig. 8 (a) HER LSVs of PtTe$_2$ as bulk crystals and as nanosheets with and without heat treatment at 200, 400, and 600 °C. (b) Corresponding Tafel lines. (c) Histogram of the overpotential at 10 mA cm$^{-2}$ and exchange current density for the same catalysts. (d) Calculated TOF at all overpotentials. (e) Plot of overpotential at 10 mA cm$^{-2}$ against the Tafel slope. (f) Nyquist plots of the same ascertaining the activity trend observed in LSVs. Reproduced with permission from ref. 93 (Copyright 2021, The Authors (published by Nature)).

with ordered Te vacancies was almost identical to metallic Pt. Besides, as PtTe$_2$ with ordered Te vacancies also had an additional boost from the undercoordinated Pt atoms from the edge-sites, it was able to surpass the HER activity of Pt/C at all overpotentials. Intriguingly, PtTe$_2$ with ordered Te vacancies did also show higher TOF and excellent cycling and potentiostatic electrolysis stabilities which were superior to Pt/C. Ping and co-workers,[94] in their recent work, demonstrated that 5–20
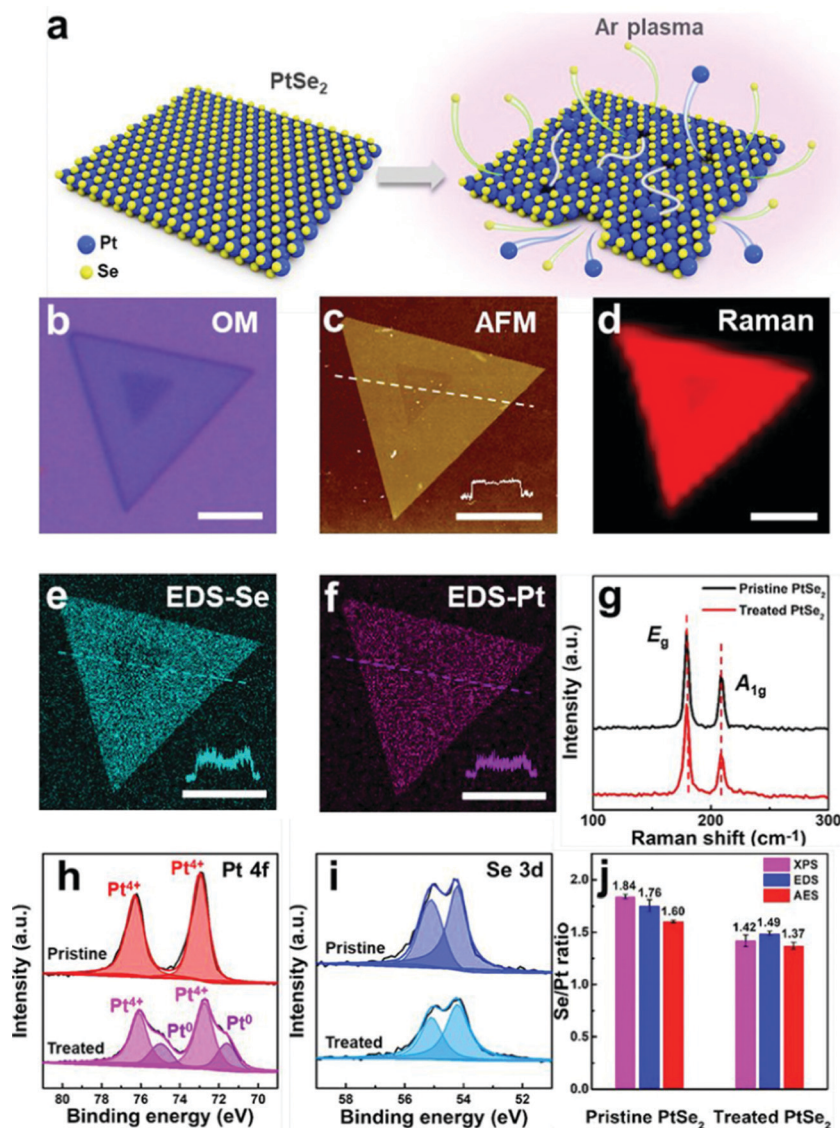
This journal is © The Royal Society of Chemistry 2022

Energy Environ. Sci., 2022, 15, 1461–1478 | 1469

Fig. 9   (a) Graphic showing the Ar-plasma etching induced creation of atomic vacancies and Pt clusters on $PtSe_2$. (b–d) The optical image, AFM images, and Raman map of a single $PtSe_2$ flake after etching. (e and f) EDS map of Se and Pt. (g) Raman spectrum of the same. (h and i) XPS narrow scans of Pt 4f and Se 3d levels of Pt and Se in $PtSe_2$ before and after Ar-plasma treatment. (j) Histogram showing the Se/Pt ratio of $PtSe_2$ before and after Ar-plasma treatment as revealed by XPS, EDS, and AES showing the increase in Pt content after treatment. Reproduced with permission from ref. 94 (Copyright 2021, American Chemical Society).

layers of 1T $PtSe_2$ flakes synthesized by their chemical vapor transport method can be engineered by irradiating the flakes with a mild Ar-plasma (5–15 W) to have atomic vacancies (both Pt and Te) and Pt clusters. These $PtSe_2$ flakes with atomic vacancies and Pt clusters were found to perform as well as Pt. From this study, it was also revealed that the increasing time of plasma irradiation increased its HER activity. Advanced spectroscopic and microscopic analyses carried out in this work have explicitly shown that there was metallic Pt after Ar-plasma treatment (Fig. 9a–j). Hence, it can safely be concluded here that no matter how fancy the structural and electronic properties of $PtX_2$ sound, they will always be poorer electrocatalytic interfaces for the HER unless otherwise there will be some special pre-treatments (such as defect engineering and

increasing the number of layers) enhancing their Pt-like characteristics. Table 1 summarizes the recent $PtX_2$ HER electrocatalysts reported in the literature in the ascending order of their overpotentials at benchmarking conditions (*i.e.*, apparent activity).

From Table 1, it is once again witnessed that $PtX_2$ (also other Pt-based chalcogenides) are poorer catalysts for the HER when compared to Pt/C unless otherwise they have additional metals, Pt heterophase, and vacancies that can result in Pt-like undercoordinated Pt sites, and metallic Pt clusters. Hence, it is apparent that to design and apply a Pt-based HER electrocatalyst ($PtX_2$) that would never have a comparable performance to that of Pt is of least practical meaning.

**Table 1** Electrocatalytic HER activity trends with $PtX_2$ catalysts in the ascending order of their overpotential at 10 mA cm$^{-2}$ (apparent activity)

| Catalyst | Medium | $\eta^{10}$/mV | Tafel slope/mV dec$^{-1}$ | Loading/mg cm$^{-2}$ | Ref. |
|---|---|---|---|---|---|
| PtSe$_2$ with vacancies and Pt clusters | 0.5 M H$_2$SO$_4$ | 11 | 48 | N/A | Ping et al.[94] |
| PtTe$_2$ with Te vacancy | 0.5 M H$_2$SO$_4$ | 22 | 29.9 | 0.809 | Li et al.[93] |
| Pt/PtTe$_2$/NiCoTe$_2$/NPFC HFSs | 0.5 M H$_2$SO$_4$ | 34 | 81 | N/A | Yi et al.[79] |
| PtPdRuTe | 0.5 M H$_2$SO$_4$ | 39 | 32 | 0.285 | Liu et al.[78] |
| PtSe$_2$/Pt | 0.5 M H$_2$SO$_4$ | 42 | 53 | N/A | Wang et al.[81] |
| PtS$_2$ QDs on TiC | 0.5 M H$_2$SO$_4$ | 55 | 60 | N/A | Jeong et al.[80] |
| PtSe$_2$ 20L | 0.5 M H$_2$SO$_4$ | 60 | 41 | N/A | Hu et al.[92] |
| Pt$_3$Bi$_2$S$_2$ | 0.5 M H$_2$SO$_4$ | 61 | 51 | N/A | Fang et al.[95] |
| 1TPtSe$_2$/CC | 0.5 M H$_2$SO$_4$ | 177 | 67 | N/A | Zhang et al.[77] |
| PtSe$_2$ 2L | 0.5 M H$_2$SO$_4$ | 200 | 92 | N/A | Hu et al.[92] |
| PtSe$_2$ film (76.0 nm) | 0.5 M H$_2$SO$_4$ | 280 | 47 | N/A | Lin et al.[76] |
| PtSe$_2$ film (57.6 nm) | 0.5 M H$_2$SO$_4$ | 320 | 63 | N/A | Lin et al.[76] |
| PtSe$_2$ film (38.0 nm) | 0.5 M H$_2$SO$_4$ | 380 | 47 | N/A | Lin et al.[76] |
| PtSe$_2$ film (19.0 nm) | 0.5 M H$_2$SO$_4$ | 450 | 60 | N/A | Lin et al.[76] |
| PtSe$_2$ film (11.4 nm) | 0.5 M H$_2$SO$_4$ | 510 | 32 | N/A | Lin et al.[76] |
| PtTe$_2$ | 0.5 M H$_2$SO$_4$ | 540 | 110 | N/A | Chia et al.[39] |
| PtSe$_2$ 1L | 0.5 M H$_2$SO$_4$ | 550 | 140 | N/A | Hu et al.[92] |
| PtSe$_2$ film (7.6 nm) | 0.5 M H$_2$SO$_4$ | 575 | 43 | N/A | Lin et al.[76] |
| PtSe$_2$ film (3.8 nm) | 0.5 M H$_2$SO$_4$ | 590 | 50 | N/A | Lin et al.[76] |
| PtSe$_2$ film (1.9 nm) | 0.5 M H$_2$SO$_4$ | 615 | 60 | N/A | Lin et al.[76] |
| PtSe$_2$ | 0.5 M H$_2$SO$_4$ | 630 | 132 | N/A | Chia et al.[39] |
| PtS$_2$ | 0.5 M H$_2$SO$_4$ | 860 | 216 | N/A | Chia et al.[39] |
| PtPdRuTe | 1.0 M KOH | 22 | 22 | 0.285 | Liu et al.[78] |
| Pt/PtTe$_2$/NiCoTe$_2$/NPFC HFSs | 1.0 M KOH | 43 | 161 | N/A | Yi et al.[79] |
| Pt/PtTe$_2$/NiCoTe$_2$/NPFC HFSs | 1.0 M PBS | 36 | 80 | N/A | Yi et al.[79] |

Note: N/A implies that the corresponding data are not available in cited reports.

It is understood from the reports on $PtX_2$ that all the attempts made to make $PtX_2$ an efficient HER catalysts were mainly due to its structural resemblance to two of the most widely studied TMDs in HER electrocatalysis (which are $WX_2$ and $MoX_2$). A quick literature survey on the recent HER reports using $WX_2$ and $MoX_2$ as electrocatalysts revealed the following key points on their activity trends. Both $MoX_2$ and $WX_2$ deliver the benchmarking current density (apparent activity) at 10 mA cm$^{-2}$ in the overpotential range of 150 to 300 V and always and almost follow the Volmer–Heyrovský mechanism with a Tafel slope ranging from 60 to 120 mV dec$^{-1}$ in both acid and alkaline solutions. The Tafel slope values tend to be closer to 120 mV dec$^{-1}$ in alkaline medium as the rate-determining step is usually the water dissociation coupled proton adsorption and discharge unlike the simple proton adsorption and discharge in acidic conditions. Due to the coupled water dissociation in the Volmer step in alkaline conditions, it is also common to witness abnormal Tafel slopes (>120 mV dec$^{-1}$). In order to compare the performance of $PtX_2$ catalysts listed in Table 1, a collection of recent $MoX_2$ and $WX_2$ catalysts are benchmarked based on their reported apparent activity in Table 2. It is advised here that the readers should be mindful of the effects of surface area, loading, and screening conditions all of which have significant influences on apparent activity.

From Table 2, it is evident that $MoX_2$ and $WX_2$ have average overpotentials of 200 and 286 mV, respectively. Apparently, these merits are far better than those of metallic Mo and W, and hence, designing and screening $MoX_2$ and $WX_2$ for the HER in comparison with Pt/C is truly purposeful and makes sense unlike comparing $PtX_2$ with Pt/C. Also, when the activity trends of Mo/$WX_2$ are compared with that of $PtX_2$, the poorer

HER activity of pristine $PtX_2$ (with no defects, vacancies, metallic single atoms, and cluster of Pt, etc.,) is explicitly evidenced. Besides, a list of recent state-of-the-art HER electrocatalysts listed in the second part of Table 2 suggest that pristine $PtX_2$ are nowhere near good enough to be compared with the state-of-the-art despite being made of Pt. This implies that working hard on a material (in its pristine form) that will never perform better than its metallic counterpart (i.e., Pt) is simply a waste of time and resources. On the other hand, the structural engineering strategies (vacancy engineering, creating Pt clusters and single atoms, and increasing the layer numbers) reported recently show some that these $PtX_2$ materials have some potential to actually become better than Pt/C. However, the question is 'at what cost?'. One has to be mindful of the time, energy, and resources spent in creating a material that would have a comparable activity (most of the time) or a slightly better activity than Pt/C and must ask 'Is it worth it?'.

## Are we missing the bigger picture here?

Undoubtedly, any effort put forward by researchers to find highly efficient electrocatalysts for energy conversion reactions including the HER of water electrolysis deserves to be appreciated. Since Pt is the superior catalyst of all for the HER in almost all pH conditions, all the other materials made of metals other than Pt are conventionally compared with Pt/C under identical working conditions to judge them for their suitability as an alternate to Pt.[9] Similarly, there is also huge interest among researchers to lower the overall Pt content

This journal is © The Royal Society of Chemistry 2022

Energy Environ. Sci., 2022, **15**, 1461–1478 | **1471**

**Table 2**  Electrocatalytic HER activity trends with $MX_2$ and $WX_2$ catalysts in the ascending order of their overpotential at 10 mA cm$^{-2}$ (apparent activity)

| Catalyst | Medium | $\eta$10/mV | Tafel slope/mV dec$^{-1}$ | Loading/mg cm$^{-2}$ | Ref. |
|---|---|---|---|---|---|
| **$MoX_2$ HER electrocatalysts** | | | | | |
| 1T $MoTe_2$ | 0.5 M $H_2SO_4$ | 73 | 46.3 | N/A | He et al.[96] |
| $MoSe_2$–$WS_2$ | 0.5 M $H_2SO_4$ | 75 | 60 | N/A | Vikraman et al.[61] |
| 1T-2H $MoSe_2$/graphene | 0.5 M $H_2SO_4$ | 98 | 49 | N/A | Deng et al.[97] |
| N-Doped $MoS_2$ | 0.5 M $H_2SO_4$ | 108 | 37 | 0.5 | Bolar et al.[98] |
| $MoS_2$–$WSe_2$ | 0.5 M $H_2SO_4$ | 116 | 76 | N/A | Vikraman et al.[99] |
| Graphene wrapped $MoS_2$ | 0.5 M $H_2SO_4$ | 118 | 73 | N/A | Nguyen et al.[100] |
| $MoSe_2$ with vacancies | 0.5 M $H_2SO_4$ | 125 | 35 | N/A | Xia et al.[101] |
| $MoS_2$–$WS_2$ heterostructure | 0.5 M $H_2SO_4$ | 129 | 72 | N/A | Vikraman et al.[102] |
| Se-Rich $MoSe_2$ | 0.5 M $H_2SO_4$ | 130 | 46 | N/A | Kwon et al.[47] |
| $MoS_2$–$WTe_2$ | 0.5 M $H_2SO_4$ | 140 | 40 | 1.2 | Zhou et al.[84] |
| $MoSe_2$–$MoO_2$ | 0.5 M $H_2SO_4$ | 142 | 48.9 | N/A | Jian et al.[103] |
| 3D $MoS_2$/graphene | 0.5 M $H_2SO_4$ | 143 | 71 | 0.5 | Meng et al.[104] |
| Disordered 1T $MoSe_2$ | 0.5 M $H_2SO_4$ | 152 | 52 | 0.14 | Yin et al.[105] |
| $MoS_2$ Moiré superlattice | 0.5 M $H_2SO_4$ | 153 | 73 | N/A | Jiang et al.[106] |
| $MOS_2$ nanomesh | 0.5 M $H_2SO_4$ | 160 | 46 | N/A | Yin et al.[107] |
| $MoSe_2$–$MoS_2$ | 0.5 M $H_2SO_4$ | 162 | 61 | N/A | Li et al.[108] |
| Electroactivated $MoTe_2$ | 0.5 M $H_2SO_4$ | 178 | 116 | N/A | McGlynn et al.[109] |
| 2D $MoS_2$–$MoSe_2$ thin sheets | 0.5 M $H_2SO_4$ | 186 | 71 | N/A | Sharma et al.[110] |
| Pores-rich $MoS_2$ | 0.5 M $H_2SO_4$ | 190 | 163 | N/A | Zhou et al.[111] |
| Deformed $MoS_2$ | 0.5 M $H_2SO_4$ | 191 | 64 | 0.13 | Chen et al.[112] |
| Amorphous $MoS_2$ | 0.5 M $H_2SO_4$ | 210 | 42 | N/A | Wu et al.[113] |
| $WS_2$–$MoS_2$@CNT | 0.5 M $H_2SO_4$ | 212 | 50 | 0.3 | Thangasamy et al.[114] |
| $MoSe_2$ nanoflowers | 0.5 M $H_2SO_4$ | 220 | 61 | N/A | Masurkar et al.[115] |
| 1T′ $MoTe_2$/CC | 0.5 M $H_2SO_4$ | 220 | 127 | N/A | Lu et al.[116] |
| $MoSe_2$–CNT | 0.5 M $H_2SO_4$ | 245 | 49 | 0.112 | Maity et al.[117] |
| 1T′-2H $MoS_2$ edges | 0.5 M $H_2SO_4$ | 290 | 83 | N/A | Zhang et al.[52] |
| $Et_2$N-Ph–$MoS_2$ | 0.5 M $H_2SO_4$ | 348 | 75 | N/A | Benson et al.[32] |
| MoSeTe | 0.5 M $H_2SO_4$ | 410 | 62 | 0.001 | Kosmala et al.[48] |
| $MoTe_2$ | 0.5 M $H_2SO_4$ | 460 | 67 | N/A | McManus et al.[118] |
| 1T′ $MoTe_2$ | 0.5 M $H_2SO_4$ | 530 | 177 | N/A | Zhuang et al.[119] |
| 1T $MoS_2$ with defects | 1.0 M KOH | 90 | 100 | 1 | Anjum et al.[120] |
| N-Doped $MoS_2$ | 1.0 M KOH | 141 | 48 | 0.5 | Bolar et al.[98] |
| 1T-2H $MoS_2$ heterostructure | 1.0 M KOH | 260 | 65 | N/A | Wang et al.[54] |
| **$WX_2$ HER electrocatalysts** | | | | | |
| $WS_2$ with S-vacancy | 0.5 M $H_2SO_4$ | 116 | 37.9 | N/A | Zhu et al.[121] |
| $WSe_2$ 3D dendrite | 0.5 M $H_2SO_4$ | 175 | 80 | N/A | Zou et al.[87] |
| $WS_2$–graphene | 0.5 M $H_2SO_4$ | 180 | 76 | N/A | Le et al.[122] |
| $WSe_2$ films | 0.5 M $H_2SO_4$ | 189 | 72 | N/A | Li et al.[123] |
| $WS_2$ with dominant 1T phase | 0.5 M $H_2SO_4$ | 200 | 50.4 | N/A | Liu et al.[124] |
| Trigonal $WS_2$–CNT | 0.5 M $H_2SO_4$ | 205 | 84 | N/A | Guo et al.[125] |
| $WS_2$–CNT | 0.5 M $H_2SO_4$ | 210 | 59.7 | N/A | Wang et al.[126] |
| Te doped $WS_2$ | 0.5 M $H_2SO_4$ | 210 | 94 | N/A | Pan et al.[127] |
| $WSe_2$ monolayer | 0.5 M $H_2SO_4$ | 245 | 76 | N/A | Sun et al.[128] |
| Sputtered $WS_2$ | 0.5 M $H_2SO_4$ | 250 | 126.3 | N/A | Nam et al.[129] |
| $WSe_2$ nanosheets | 0.5 M $H_2SO_4$ | 275 | 78 | N/A | Wang et al.[88] |
| $WS_2$–graphdyine | 0.5 M $H_2SO_4$ | 275 | 54 | 0.29 | Yao et al.[130] |
| $WS_2$–graphite protected | 0.5 M $H_2SO_4$ | 280 | 47.9 | N/A | Yang et al.[131] |
| $WTe_2$ edges | 0.5 M $H_2SO_4$ | 325 | 96 | N/A | Ling et al.[132] |
| 1T-$WS_2$ | 0.5 M $H_2SO_4$ | 350 | 95 | N/A | Kim et al.[133] |
| $WS_2$–$WO_3$ | 0.5 M $H_2SO_4$ | 380 | 50 | 0.14 | Shang et al.[134] |
| $WSe_2$–rGO | 0.5 M $H_2SO_4$ | 390 | 85 | N/A | Liu et al.[135] |
| Edge-engineered $WS_2$ | 0.5 M $H_2SO_4$ | 390 | 122 | N/A | Shirazi et al.[136] |
| $WSe_2$–$S^{2-}$/$Na^+$ | 0.5 M $H_2SO_4$ | 400 | 97 | 1 | Kim et al.[137] |
| Semimetallic $WTe_2$ | 0.5 M $H_2SO_4$ | 450 | 57 | N/A | Hong et al.[138] |
| Te-Vacant $WTe_2$ | 0.5 M $H_2SO_4$ | 550 | 159 | N/A | Kwon et al.[139] |
| **Selected state-of-the-art in HER electrocatalysts** | | | | | |
| $Rh_2P$ | 0.5 M $H_2SO_4$ | 14 | 32 | N/A | Yang et al.[140] |
| Ru–NC | 1.0 M KOH | 17 | 32 | 0.24 | Liu et al.[141] |
| $Rh_2P$ | 0.5 M $H_2SO_4$ | 17 | 35 | 0.114 | Zhao et al.[142] |
| $NiFe_2O_4$–Ru–Ni | 1.0 M KOH | 18 | 27 | 0.1 | Niu et al.[143] |
| Pt | 0.5 M $H_2SO_4$ | 24 | 31 | N/A | Yang et al.[140] |
| Pt/C–Ni foam | 1.0 M KOH | 25 | 99 | 0.1 | Niu et al.[143] |
| Pt/C | 1.0 M KOH | 25 | 23 | 0.285 | Luo et al.[144] |
| Ru–C | 1.0 M KOH | 27 | 33 | 0.285 | Luo et al.[144] |
| Pt/C | 0.5 M $H_2SO_4$ | 27 | 32 | 0.114 | Zhao et al.[142] |
| NiFe LDH–Ru | 1.0 M KOH | 29 | 31 | N/A | Chen et al.[145] |
| $Rh_2P$ | 1.0 M KOH | 30 | 50 | N/A | Yang et al.[140] |

**Energy & Environmental Science**

**Table 2** (continued)

| Catalyst | Medium | $\eta 10$/mV | Tafel slope/mV dec$^{-1}$ | Loading/mg cm$^{-2}$ | Ref. |
|---|---|---|---|---|---|
| Pt/C | 1.0 M KOH | 31 | 32 | N/A | Chen et al.[145] |
| Pt/C | 1.0 M KOH | 32 | 32 | 0.24 | Liu et al.[141] |
| Ru–NC | 1.0 M KOH | 32 | 64 | N/A | Wang et al.[146] |
| Pt | 1.0 M PBS | 32 | 51 | N/A | Yang et al.[140] |
| Pt/C | 1.0 M KOH | 34 | N/A | N/A | Wang et al.[146] |
| Rh$_2$P | 1.0 M PBS | 38 | 46 | N/A | Yang et al.[140] |
| Pt | 1.0 M KOH | 58 | 77 | N/A | Yang et al.[140] |

Note: N/A implies that the corresponding data are not available in cited reports.

instead of replacing it completely so that one would not have to compromise activity and energy-efficiency. Nanostructuring-assisted high surface area Pt particles synthesis and their subsequent stabilization on a suitable support/substrate is an active research area.[147–149] In such cases, these low-Pt nanocatalysts are compared with Pt/C (20 wt%) to assess their superiority. In electrocatalytic water splitting, these two objectives are important as they address the issue of the scarcity of Pt. However, when a catalyst made of Pt (such as PtX$_2$) is incapable of surpassing the parent Pt or Pt/C in HER electrocatalytic activity, putting so much time and resources in this area is simply meaningless. From the above discussion and Tables 1 and 2, it could have been witnessed that even MoX$_2$ and WX$_2$ deliver better HER performances than pristine PtX$_2$. To get a clear picture of the HER activity trends of MoX$_2$, WX$_2$, and PtX$_2$ in comparison with Pt/C, the average overpotential at 10 mA cm$^{-2}$ required by all these materials (an average of the values from cited reports and there could significant deviation when just a single study is considered) are plotted as a histogram (Fig. 10). From Fig. 10, it is once again proven that working with PtX$_2$ for the purpose of applying it to HER when

we have a better catalyst comprised of the same Pt (Pt/C) for the same is essentially meaningless. Moreover, even when PtX$_2$ with undercoordinated Pt sites, Pt clusters, and other metals are put to the job of the HER, their average overpotential at 10 mA cm$^{-2}$ remains still higher than that of Pt/C. Since we cannot completely criticise the advantages of PtX$_2$ that it may have in HER electrocatalysis, we looked into other facts in which PtX$_2$ can actually be better than Pt. The main advantage with PtX$_2$ (that too only with the monolayers of PtX$_2$) is the 100% accessibility of Pt sites unlike the solid Pt electrodes. Hence, if the activity is reported in mA Pt$^{-1}$, PtX$_2$ can surely deliver better activity than Pt as only the surface sites are available for the HER with the latter one. To show this, we took the data reported by Chia and co-workers and converted it into activity per Pt site (Fig. 11a–c). The number of Pt sites was calculated from the lattice parameters of Pt, PtS$_2$, PtSe$_2$, and PtTe$_2$.

Fig. 11a shows the as-adopted data with activity normalized by geometrical area. Fig. 11b on the other hand shows the activity normalized by the number of Pt sites. Clearly, PtX$_2$ delivered several orders of magnitudes of activity (in mA Pt$^{-1}$) higher than Pt as shown in Fig. 11c. However, one should also note here that irrespective of the high activity per Pt sites, the onset potential remains the same indicating that Pt has the upper hand when it comes to practical electrolysis. Hence, the higher activity per Pt site shown in Fig. 11b and c is useless unless the same can be capitalized into apparent activity. Other than these observations, the following are also the reasons why PtX$_2$ could never outperform Pt in practical electrolysis of water in its pristine form.

● 100% accessibility of Pt sites is possible with only monolayer PtX$_2$. However, the experimental studies suggest that monolayer PtX$_2$ (in sharp contrast to that of Mo/WX$_2$) catalyze the HER poorly compared with those with higher layer numbers. This is mainly because all the Pt atoms accessed in monolayer PtX$_2$ are actually Pt$^{4+}$ ions. The density of states (DOS) of Pt$^{4+}$ ions are quite different from those of Pt$^0$ and do not possess a HER favoring band structure (please refer to our discussion on the role of DOS on HER activity).

● Only PtX$_2$ catalysts with vacancies and defects that led to the formation of metallic Pt single atoms and clusters performed better and possessed a comparable activity to that of Pt/C. This indicates that having metallic Pt is more important than ensuring 100% accessibility in the form of Pt$^{4+}$.

● Because of such differences in DOS, pristine PtX$_2$ have always had a higher onset overpotential (even higher than Mo/WX$_2$) for the HER than Pt/C. This basically undermines the
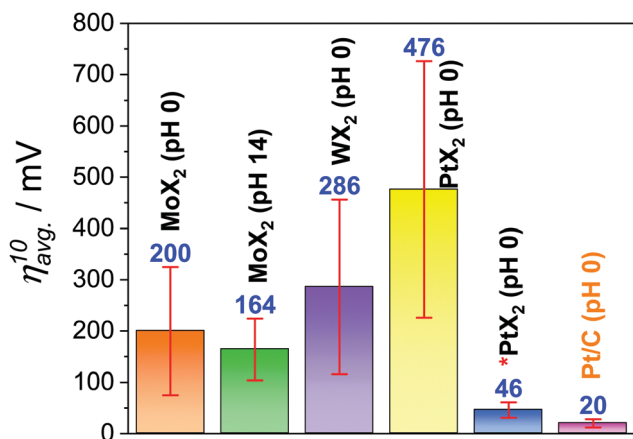


**Fig. 10** Histogram of the average overpotential at 10 mA cm$^{-2}$ (apparent activity) required by MoX$_2$, WX$_2$, pristine PtX$_2$, and Pt/C pH 0 with MoX$_2$ in pH 14 (green bar) showing the superiority of Pt/C over PtX$_2$. The asterisk symbol indicates that these PtX$_2$ catalysts had assistance from other contributors like undercoordinated Pt-sites, more layer numbers, vacancies leading to the formation of Pt clusters, other highly active materials, and having an additional Pt heterointerface. Each $\eta_{avg.}^{10}$ value is the average one calculated using the data from multiple reports in Tables 1 and 2.

This journal is © The Royal Society of Chemistry 2022

Energy Environ. Sci., 2022, **15**, 1461–1478 | **1473**
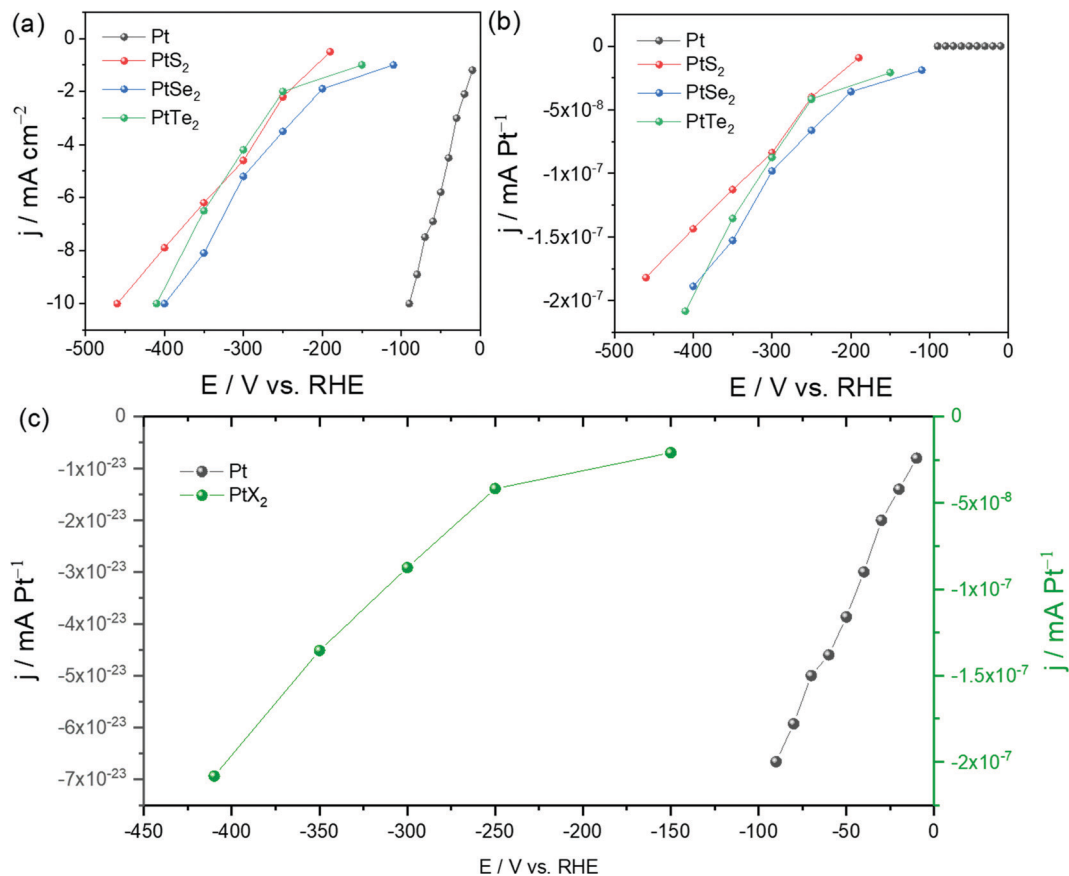
**Fig. 11** (a) Activity of PtX$_2$ catalysts in comparison with Pt as reported by Chia and co-workers.[39] (b) The activity of the same catalysts normalized by the number of Pt Sites. (c) Number of Pt sites normalized activity of PtTe$_2$ and Pt showing several orders of magnitudes of difference but with the same onset potentials implying that Pt is still superior to PtX$_2$ in intrinsic activity (so is in apparent activity). Note: The values of activity were manually read from the figures given by the original study by Chia and co-workers[39] and there could be some deviations in the data points. Hence, the readers are solicited to act on their own discretion.

goals of HER electrocatalysis. In other words, there is no meaning in ensuring 100% accessibility when we need to trade off the onset overpotential to a greater extent.

From the above discussion, we can say 'We Are Missing the Bigger Picture Here'. However, it should not be left without mentioning that the reports published on the HER activity trends of PtX$_2$ catalysts have helped us to understand the structure–activity relationship in PtX$_2$ as well as in other MX$_2$ catalysts. Hence, it is not that just that PtX$_2$ is a poor catalyst for HER, it is totally useless. It could be useful and actually be better than Pt in other areas of applications. Hence, it is concluded here that in HER electrocatalysis, the bigger picture (finding an alternate with comparable activity to Pt and lowering the total Pt content without compromising its HER activity) should not be missed.

## Conclusions and outlook

HER electrocatalysis is an important area of water electrolysis research that focuses mainly on three goals. (1) Replacing Pt entirely with a non-Pt catalyst for HER, with a non-Pt catalyst,

(2) lowering the total Pt content without making any compromise in activity, and (3) improving the poor kinetics of Pt in alkaline conditions. With all these goals, any progress made is conventionally compared with that of Pt/C under identical experimental conditions as it is the state-of-the-art to date. In studies where Pt-based catalysts are engineered structurally to lower the total Pt content and improve its kinetics, they are expected to surpass the commercial Pt/C in terms of both activity and HER kinetics. With PtX$_2$, it appears that this basic requisite has been forgotten. Pristine PtX$_2$ with an average overpotential of 476 mV (calculated from the works cited in this study and could vary notably but not extensively depending on the studies that may emerge in the future) at 10 mA cm$^{-2}$ is nowhere near the performance delivered by Pt/C which is basically undermining the whole objective of designing and applying a material for the HER electrocatalyst. On the other hand, PtX$_2$ that had assistance from other factors listed above performed better yet still poorer than Pt/C on average. Hence, it is time that we stop and question ourselves 'Are we doing it right?'. However, it is unanimously agreed here that new knowledge added by the studies on the activity trend of PtX$_2$ and the correlations that were made with the activity trends of

other $MX_2$ materials in comparison with $PtX_2$ is invaluable. Similarly, since a monolayer $PtX_2$ ensures 100% accessibility to all the Pt sites and $PtX_2$ with more layers to a notable extent than one can access with Pt/C, the activity reported per Pt atom could actually add weightage to $PtX_2$-based HER catalysts over the same reported for Pt/C. However, it should be reminded here that all the sites that are accessed with $PtX_2$ are tetravalent Pt cations ($Pt^{4+}$) and not metallic Pt. These two have very distinct electronic structures and DOS population at and around 0.0 eV which suggests that only metallic Pt has an appropriate electronic structure for facile HER electrocatalysis on its surface. Hence, it may not matter how much percentage of Pt we can access as long as the accessed Pt site is chemically different from metallic Pt and will always have a poorer HER activity (as evidenced from the higher onset overpotentials of $PtX_2$ in the HER). The huge anticipation laid on $PtX_2$ to have a better HER performance was mainly because it is isostructural to $Mo/WX_2$ HER electrocatalysts. However, $Mo/WX_2$ are very different in their electronic properties linked to HER activity and have an inverse trend of activity with the increasing number of layers. This is one of many reasons why the theoretical predictions about $PtX_2$ failed in experimental studies. This implies that both theoretical and experimental studies should go hand in hand in order to identify, justify, and resolve any hurdles that may be encountered in the way of developing a better catalyst while being complementary to one another.

Despite the humongous issues pointed out in this perspective, we will not recommend abandoning $PtX_2$ completely. Instead, these graphene-like and structurally intriguing $PtX_2$ can be used as synergistic supports and pre-catalysts. It has been shown that electrochemical cycling and potentiostatic/galvanostatic electrolysis can activate $PtX_2$ towards the HER by lowering the demanded overpotential significantly. Key insights of such studies indicate that such electroactivation results in the formation of metallic Pt clusters and nanoparticles on the $PtX_2$ matrix while leaving multiple vacancies behind which in turn resulted in undercoordinated metallic Pt-like Pt atomic sites. This can be used as a potential way to enhance the activity of $PtX_2$ so that it could outperform Pt/C as demonstrated by a few already. However, high activity realized just by (single atom) vacancy engineering cannot be a long-term solution, as these vacancies are highly prone to the restructuring of the local environment around it particularly when the working condition is reductive in nature. Other options that are available with $PtX_2$ are heterostructuring and doping metallic Pt clusters and particles so that one could lower the total content yet can have a better performance than Pt/C. Other than this application (HER)-oriented prospects, $PtX_2$ can become a useful model catalyst to study the structure–activity relationship and elucidating mechanism of the HER in comparison with other $MX_2$ HER electrocatalysts. If not, spending time and resources just to create a poorly active HER electrocatalyst ($PtX_2$) out of the state-of-the-art (Pt) is unfortunately and undeniably meaningless.

## Conflicts of interest

There are no conflicts to declare.

## Acknowledgements

## References

1 M.-R. Gao, Y.-F. Xu, J. Jiang and S.-H. Yu, *Chem. Soc. Rev.*, 2013, **42**, 2986–3017.

2 Y. Jiao, Y. Zheng, M. Jaroniec and S. Z. Qiao, *Chem. Soc. Rev.*, 2015, **44**, 2060–2086.

3 S. Anantharaj, S. R. Ede, K. Sakthikumar, K. Karthick, S. Mishra and S. Kundu, *ACS Catal.*, 2016, **6**, 8069–8097.

4 S. Anantharaj and V. Aravindan, *Adv. Energy Mater.*, 2019, **2**, 1902666.

5 S. Anantharaj and S. Noda, *Small*, 2020, **16**, 1905779.

6 Y. Shi and B. Zhang, *Chem. Soc. Rev.*, 2016, **45**, 1529–1541.

7 S. Anantharaj, *J. Mater. Chem. A*, 2021, **9**, 6710–6731.

8 S. Anantharaj, S. Noda, V. R. R. Jothi, S. C. Yi, M. Driess and P. W. Menezes, *Angew. Chem., Int. Ed.*, 2021, **60**(35), 18981–19006, DOI: 10.1002/anie.202015738.

9 S. Anantharaj, S. Kundu and S. Noda, *J. Mater. Chem. A*, 2020, 4174–4192.

10 N. Dubouis and A. Grimaud, *Chem. Sci.*, 2019, **10**, 9165–9181.

11 M. Miao, J. Pan, T. He, Y. Yan, B. Y. Xia and X. Wang, *Chem. – Eur. J.*, 2017, **23**, 10947–10961.

12 W. Luo, Y. Wang and C. Cheng, *Mater. Today Phys.*, 2020, **15**, 100274.

13 Y. Yan, B. Xia, Z. Xu and X. Wang, *ACS Catal.*, 2014, **4**, 1693–1705.

14 P. Xiao, W. Chen and X. Wang, *Adv. Energy Mater.*, 2015, **5**, 1500985.

15 D. Strmcnik, P. P. Lopes, B. Genorio, V. R. Stamenkovic and N. M. Markovic, *Nano Energy*, 2016, **29**, 29–36.

16 Y. Zheng, Y. Jiao, A. Vasileff and S. Z. Qiao, *Angew. Chem., Int. Ed.*, 2018, **57**, 7568–7579.

17 J. Wang, W. Cui, Q. Liu, Z. Xing, A. M. Asiri and X. Sun, *Adv. Mater.*, 2016, **28**, 215–230.

18 Q. Liu, Z. Pu, A. M. Asiri and X. Sun, *Electrochim. Acta*, 2014, **149**, 324–329.

19 J. Tian, Q. Liu, Y. Liang, Z. Xing, A. M. Asiri and X. Sun, *ACS Appl. Mater. Interfaces*, 2014, **6**, 20579–20584.

20 P. Jiang, Q. Liu, Y. Liang, J. Tian, A. M. Asiri and X. Sun, *Angew. Chem., Int. Ed.*, 2014, **53**, 12855–12859.

21 J. Tian, Q. Liu, Y. Liang, Z. Xing, A. M. Asiri and X. Sun, *ACS Appl. Mater. Interfaces*, 2014, **6**, 20579–20584.

22 Y. Liang, Q. Liu, A. M. Asiri, X. Sun and Y. Luo, *ACS Catal.*, 2014, **4**, 4065–4069.

23 J. Park, B. Koo, K. Y. Yoon, Y. Hwang, M. Kang, J. G. Park and T. Hyeon, *J. Am. Chem. Soc.*, 2005, **127**, 8433–8440.

This journal is © The Royal Society of Chemistry 2022

*Energy Environ. Sci.*, 2022, **15**, 1461–1478 | **1475**

24 J. F. Callejas, C. G. Read, C. W. Roske, N. S. Lewis and R. E. Schaak, *Chem. Mater.*, 2016, **28**(17), 6017–6044, DOI: 10.1021/acs.chemmater.6b02148.

25 J. Kibsgaard, C. Tsai, K. Chan, J. D. Benck, J. K. Nørskov, F. Abild-Pedersen and T. F. Jaramillo, *Energy Environ. Sci.*, 2015, **8**, 3022–3029.

26 A. E. Henkes, Y. Vasquez and R. E. Schaak, *J. Am. Chem. Soc.*, 2007, **129**, 1896–1897.

27 S. Anantharaj, S. R. Ede, K. Sakthikumar, K. Karthick, S. Mishra and S. Kundu, *ACS Catal.*, 2016, **6**, 8069–8097.

28 S. Anantharaj, E. Subhashini, K. C. Swaathini, T. S. Amarnath, S. Chatterjee, K. Karthick and S. Kundu, *Appl. Surf. Sci.*, 2019, **487**, 1152–1158.

29 X. Chia, Z. Sofer, J. Luxa and M. Pumera, *ACS Appl. Mater. Interfaces*, 2017, **9**, 25587–25599.

30 J. Luxa, P. Vosecký, V. Mazánek, D. Sedmidubský, M. Pumera, P. Lazar and Z. Sofer, *ACS Catal.*, 2017, **7**, 5706–5716.

31 D. Voiry, J. Yang and M. Chhowalla, *Adv. Mater.*, 2016, **28**, 6197–6206.

32 E. E. Benson, H. Zhang, S. A. Schuman, S. U. Nanayakkara, N. D. Bronstein, S. Ferrere, J. L. Blackburn and E. M. Miller, *J. Am. Chem. Soc.*, 2018, **140**, 441–450.

33 W. L. Tao, Y. Q. Zhao, Z. Y. Zeng, X. R. Chen and H. Y. Geng, *ACS Appl. Mater. Interfaces*, 2021, **13**, 8700–8709.

34 X.-W. Tong, J.-J. Wang, J.-X. Li, X.-F. Hu, D. Wu and L.-B. Luo, *Sens. Actuators, A*, 2021, **322**, 112625.

35 Y. Shan, T. Li and L. Liu, *Phys. E*, 2020, **116**, 113741.

36 J. Mangin and P. Veber, *J. Cryst. Growth*, 2008, **310**, 3077–3083.

37 D. Wang, W. Ju, D. Kang, T. Li and H. Li, *Vacuum*, 2021, **183**, 109859.

38 N. Rohaizad, C. C. Mayorga-Martinez, M. Fojtů, N. M. Latiff and M. Pumera, *Chem. Soc. Rev.*, 2021, **50**, 619–657.

39 X. Chia, A. Adriano, P. Lazar, Z. Sofer, J. Luxa and M. Pumera, *Adv. Funct. Mater.*, 2016, **26**, 4306–4318.

40 J. D. Benck, T. R. Hellstern, J. Kibsgaard, P. Chakthranont and T. F. Jaramillo, *ACS Catal.*, 2014, **4**, 3957–3971.

41 Q. Ding, B. Song, P. Xu and S. Jin, *Chem*, 2016, **1**, 699–726.

42 J. Theerthagiri, R. A. Senthil, B. Senthilkumar, A. Reddy Polu, J. Madhavan and M. Ashokkumar, *J. Solid State Chem.*, 2017, **252**, 43–71.

43 P. M. Pataniya, D. Late and C. K. Sumesh, *ACS Appl. Energy Mater.*, 2021, **4**, 755–762.

44 J. Seok, J. H. Lee, S. Cho, B. Ji, H. W. Kim, M. Kwon, D. Kim, Y. M. Kim, S. H. Oh, S. W. Kim, Y. H. Lee, Y. W. Son and H. Yang, *2D Mater.*, 2017, **4**, 025061, DOI: 10.1088/2053-1583/aa659d.

45 X. Han, X. Tong, X. Liu, A. Chen, X. Wen, N. Yang and X. Y. Guo, *ACS Catal.*, 2018, **8**, 1828–1836.

46 R. K. Biroju, D. Das, R. Sharma, S. Pal, L. P. L. Mawlong, K. Bhorkar, P. K. Giri, A. K. Singh and T. N. Narayanan, *ACS Energy Lett.*, 2017, **2**, 1355–1361.

47 I. S. Kwon, I. H. Kwak, T. T. Debela, H. G. Abbas, Y. C. Park, J. P. Ahn, J. Park and H. S. Kang, *ACS Nano*, 2020, **14**, 6295–6304.

48 T. Kosmala, H. Coy Diaz, H.-P. Komsa, Y. Ma, A. V. Krasheninnikov, M. Batzill and S. Agnoli, *Adv. Energy Mater.*, 2018, **8**, 1800031.

49 S. Deng, F. Yang, Q. Zhang, Y. Zhong, Y. Zeng, S. Lin, X. Wang, X. Lu, C. Wang, L. Gu, X. Xia and J. Tu, *Adv. Mater.*, 2018, **30**, 1802223.

50 R. J. Toh, Z. Sofer, J. Luxa, D. Sedmidubský and M. Pumera, *Chem. Commun.*, 2017, **53**, 3054–3057.

51 S. Deng, M. Luo, C. Ai, Y. Zhang, B. Liu, L. Huang, Z. Jiang, Q. Zhang, L. Gu, S. Lin, X. Wang, L. Yu, J. Wen, J. Wang, G. Pan, X. Xia and J. Tu, *Angew. Chem., Int. Ed.*, 2019, **58**, 16289–16296.

52 J. Zhang, J. Wu, H. Guo, W. Chen, J. Yuan, U. Martinez, G. Gupta, A. Mohite, P. M. Ajayan and J. Lou, *Adv. Mater.*, 2017, **29**, 1701955.

53 J. M. Woods, Y. Jung, Y. Xie, W. Liu, Y. Liu, H. Wang and J. J. Cha, *ACS Nano*, 2016, **10**, 2004–2009.

54 S. Wang, D. Zhang, B. Li, C. Zhang, Z. Du, H. Yin, X. Bi and S. Yang, *Adv. Energy Mater.*, 2018, **8**, 1801345.

55 W. Zhou, M. Chen, M. Guo, A. Hong, T. Yu, X. Luo, C. Yuan, W. Lei and S. Wang, *Nano Lett.*, 2020, **20**, 2923–2930.

56 J. Zhang, X. Xu, L. Yang, D. Cheng and D. Cao, *Small Methods*, 2019, **3**, 1900653.

57 J. D. Benck, Z. Chen, L. Y. Kuritzky, A. J. Forman and T. F. Jaramillo, *ACS Catal.*, 2012, **2**, 1916–1923.

58 F. Wang, P. He, Y. Li, T. A. Shifa, Y. Deng, K. Liu, Q. Wang, F. Wang, Y. Wen, Z. Wang, X. Zhan, L. Sun and J. He, *Adv. Funct. Mater.*, 2017, **27**, 1605802.

59 Y. Jing, X. Mu, C. Xie, H. Liu, R. Yan, H. Dai, C. Liu and X. D. Zhang, *Int. J. Hydrogen Energy*, 2019, **44**, 809–818.

60 J. Wu, T. Chen, C. Zhu, J. Du, L. Huang, J. Yan, D. Cai, C. Guan and C. Pan, *ACS Sustainable Chem. Eng.*, 2020, **8**, 4474–4480.

61 D. Vikraman, S. Hussain, S. A. Patil, L. Truong, A. A. Arbab, S. H. Jeong, S. H. Chun, J. Jung and H. S. Kim, *ACS Appl. Mater. Interfaces*, 2021, **13**, 5061–5072.

62 M. S. Shawkat, J. Gil, S. S. Han, T. J. Ko, M. Wang, D. Dev, J. Kwon, G. H. Lee, K. H. Oh, H. S. Chung, T. Roy, Y. Jung and Y. Jung, *ACS Appl. Mater. Interfaces*, 2020, **12**, 14341–14351.

63 K. A. Persson, B. Waldwick, P. Lazic and G. Ceder, *Phys. Rev. B: Condens. Matter Mater. Phys.*, 2012, **85**, 235438.

64 J. N. Hansen, H. Prats, K. K. Toudahl, N. Mørch Secher, K. Chan, J. Kibsgaard and I. Chorkendorff, *ACS Energy Lett.*, 2021, **6**, 1175–1180.

65 Y. Cheng, S. Lu, F. Liao, L. Liu, Y. Li and M. Shao, *Adv. Funct. Mater.*, 2017, **27**, 1700359.

66 S. Anantharaj, S. R. Ede, K. Karthick, S. Sam Sankar, K. Sangeetha, P. E. Karthik, S. Kundu, E. K. Pitchiah and S. Kundu, *Energy Environ. Sci.*, 2018, **11**, 744–771.

67 M. Gong, D. Y. Wang, C. C. Chen, B. J. Hwang and H. Dai, *Nano Res.*, 2016, **9**, 28–46.

68 S. Anantharaj and S. Kundu, *ACS Energy Lett.*, 2019, **4**, 1260–1264.

69 S. Anantharaj, P. E. Karthik and S. Noda, *Angew. Chem., Int. Ed.*, 2021, **60**, 23051–23067.

70 S. Anantharaj, S. Noda, M. Driess and P. W. Menezes, *ACS Energy Lett.*, 2021, **6**, 1607–1611.

1476 | *Energy Environ. Sci.*, 2022, **15**, 1461–1478

This journal is © The Royal Society of Chemistry 2022

71 C. Tsai, K. Chan, J. K. Nørskov and F. Abild-Pedersen, *Surf. Sci.*, 2015, **640**, 133–140.

72 S. H. Mir, S. Chakraborty, J. Wärnå, S. Narayan, P. C. Jha, P. K. Jha and R. Ahuja, *Catal. Sci. Technol.*, 2017, **7**, 687–692.

73 J. Liu, H. Xu, J. Yan, J. Huang, Y. Song, J. Deng, J. Wu, C. Ding, X. Wu, S. Yuan and H. Li, *J. Mater. Chem. A*, 2019, **7**, 18906–18914.

74 H. Huang, X. Fan, D. J. Singh and W. Zheng, *ACS Omega*, 2018, **3**, 10058–10065.

75 L. J. Ma and H. Shen, *Appl. Surf. Sci.*, 2021, **545**, 149013.

76 S. Lin, Y. Liu, Z. Hu, W. Lu, C. H. Mak, L. Zeng, J. Zhao, Y. Li, F. Yan, Y. H. Tsang, X. Zhang and S. P. Lau, *Nano Energy*, 2017, **42**, 26–33.

77 L. Zhang, D. Kong, Q. Zhuang, M. Wang, T. Zhang, J. Zang, W. Shen, T. Xu, D. Wu, Y. Tian, Y. Wang, X. Li and X. Huang, *J. Mater. Chem. C*, 2021, **9**, 9524–9531.

78 S. Liu, X. Mu, W. Li, M. Lv, B. Chen, C. Chen and S. Mu, *Nano Energy*, 2019, **61**, 346–351.

79 M. Yi, S. Hu, B. B. Lu, N. Li, Z. Zhu, X. Huang, M. Wang and J. Zhang, *J. Alloys Compd.*, 2021, **884**, 161042, DOI: 10.1016/j.jallcom.2021.161042.

80 S. Jeong, H. D. Mai, T. K. Nguyen, J. S. Youn, K. H. Nam, C. M. Park and K. J. Jeon, *Appl. Catal., B*, 2021, **293**, 120227.

81 Z. Wang, B. Xiao, Z. Lin, Y. Xu, Y. Lin, F. Meng, Q. Zhang, L. Gu, B. Fang, S. Guo and W. Zhong, *Angew. Chem.*, 2021, **60**(43), 23388–23393, DOI: 10.1002/ange.202110335.

82 D. Voiry, H. Yamaguchi, J. Li, R. Silva, D. C. B. Alves, T. Fujita, M. Chen, T. Asefa, V. B. Shenoy, G. Eda and M. Chhowalla, *Nat. Mater.*, 2013, **12**, 850–855.

83 D. Escalera-López, R. Griffin, M. Isaacs, K. Wilson, R. E. Palmer and N. V. Rees, *Appl. Mater. Today*, 2018, **11**, 70–81.

84 Y. Zhou, J. V. Pondick, J. L. Silva, J. M. Woods, D. J. Hynek, G. Matthews, X. Shen, Q. Feng, W. Liu, Z. Lu, Z. Liang, B. Brena, Z. Cai, M. Wu, L. Jiao, S. Hu, H. Wang, C. M. Araujo and J. J. Cha, *Small*, 2019, **15**, 1900078.

85 D. Xu, P. Xu, Y. Zhu, W. Peng, Y. Li, G. Zhang, F. Zhang, T. E. Mallouk and X. Fan, *ACS Appl. Mater. Interfaces*, 2018, **10**, 2810–2818.

86 X. Zhou, Y. Liu, H. Ju, B. Pan, J. Zhu, T. Ding, C. Wang and Q. Yang, *Chem. Mater.*, 2016, **28**, 1838–1846.

87 M. Zou, J. Zhang, H. Zhu, M. Du, Q. Wang, M. Zhang and X. Zhang, *J. Mater. Chem. A*, 2015, **3**, 12149–12153.

88 X. Wang, Y. Chen, B. Zheng, F. Qi, J. He, Q. Li, P. Li and W. Zhang, *J. Alloys Compd.*, 2017, **691**, 698–704.

89 X. Zhang, L. Li, Y. Guo, D. Liu and T. You, *J. Colloid Interface Sci.*, 2016, **472**, 69–75.

90 J. Xie, H. Qu, J. Xin, X. Zhang, G. Cui, X. Zhang, J. Bao, B. Tang and Y. Xie, *Nano Res.*, 2017, **10**, 1178–1188.

91 R. A. B. Villaos, C. P. Crisostomo, Z.-Q. Huang, S.-M. Huang, A. A. B. Padama, M. A. Albao, H. Lin and F.-C. Chuang, *npj 2D Mater. Appl.*, 2019, **3**, 1–8.

92 D. Hu, T. Zhao, X. Ping, H. Zheng, L. Xing, X. Liu, J. Zheng, L. Sun, L. Gu, C. Tao, D. Wang and L. Jiao, *Angew. Chem.*, 2019, **131**, 7051–7055.

93 X. Li, Y. Fang, J. Wang, H. Fang, S. Xi, X. Zhao, D. Xu, H. Xu, W. Yu, X. Hai, C. Chen, C. Yao, H. B. Tao, A. G. R. Howe, S. J. Pennycook, B. Liu, J. Lu and C. Su, *Nat. Commun.*, 2021, **12**, 2351.

94 X. Ping, D. Liang, Y. Wu, X. Yan, S. Zhou, D. Hu, X. Pan, P. Lu and L. Jiao, *Nano Lett.*, 2021, **21**, 3857–3863.

95 Y. Fang, S. Wang, G. Lin, X. Wang and F. Huang, *Chem. Commun.*, 2021, **57**, 7946–7949.

96 Y. He, M. Boubeche, Y. Zhou, D. Yan, L. Zeng, X. Wang, K. Yan and H. Luo, *J. Phys. Mater.*, 2020, **4**, 014001.

97 S. Deng, Y. Zhong, Y. Zeng, Y. Wang, Z. Yao, F. Yang, S. Lin, X. Wang, X. Lu, X. Xia and J. Tu, *Adv. Mater.*, 2017, **29**, 1700748.

98 S. Bolar, S. Shit, N. C. Murmu and T. Kuila, *ChemElectroChem*, 2020, **7**, 336–346.

99 D. Vikraman, S. Hussain, L. Truong, K. Karuppasamy, H. J. Kim, T. Maiyalagan, S. H. Chun, J. Jung and H. S. Kim, *Appl. Surf. Sci.*, 2019, **480**, 611–620.

100 V. T. Nguyen, P. A. Le, Y. C. Hsu and K. H. Wei, *ACS Appl. Mater. Interfaces*, 2020, **12**, 11533–11542.

101 B. Xia, T. Wang, X. Jiang, T. Zhang, J. Li, W. Xiao, P. Xi, D. Gao, D. Xue and J. Ding, *ACS Energy Lett.*, 2018, **3**, 2167–2172.

102 D. Vikraman, S. Hussain, K. Akbar, L. Truong, A. Kathalingam, S. H. Chun, J. Jung, H. J. Park and H. S. Kim, *ACS Sustainable Chem. Eng.*, 2018, **6**, 8400–8409.

103 C. Jian, Q. Cai, W. Hong, J. Li and W. Liu, *Small*, 2018, **14**, 1703798.

104 X. Meng, L. Yu, C. Ma, B. Nan, R. Si, Y. Tu, J. Deng, D. Deng and X. Bao, *Nano Energy*, 2019, **61**, 611–616.

105 Y. Yin, Y. Zhang, T. Gao, T. Yao, X. Zhang, J. Han, X. Wang, Z. Zhang, P. Xu, P. Zhang, X. Cao, B. Song and S. Jin, *Adv. Mater.*, 2017, **29**, 1700311.

106 Z. Jiang, W. Zhou, A. Hong, M. Guo, X. Luo and C. Yuan, *ACS Energy Lett.*, 2019, 2830–2835.

107 Y. Li, K. Yin, L. Wang, X. Lu, Y. Zhang, Y. Liu, D. Yan, Y. Song and S. Luo, *Appl. Catal., B*, 2018, **239**, 537–544.

108 S. Li, W. Zang, X. Liu, S. J. Pennycook, Z. Kou, C. Yang, C. Guan and J. Wang, *Chem. Eng. J.*, 2019, **359**, 1419–1426.

109 J. C. McGlynn, T. Dankwort, L. Kienle, N. A. G. Bandeira, J. P. Fraser, E. K. Gibson, I. Cascallana-Matías, K. Kamarás, M. D. Symes, H. N. Miras and A. Y. Ganin, *Nat. Commun.*, 2019, **10**, 4916.

110 M. D. Sharma, C. Mahala and M. Basu, *Inorg. Chem.*, 2020, **59**, 4377–4388.

111 Q. Zhou, X. Luo, Y. Li, Y. Nan, H. Deng, E. Ou and W. Xu, *Int. J. Hydrogen Energy*, 2020, **45**, 433–442.

112 Y. Chen, A. Lu, P. Lu, X. Yang, C. Jiang, M. Mariano, B. Kaehr, O. Lin, A. Taylor, I. D. Sharp, L. Li, S. S. Chou and V. Tung, *Adv. Mater.*, 2017, **29**, 1703863.

113 L. Wu, A. Longo, N. Y. Dzade, A. Sharma, M. M. R. M. Hendrix, A. A. Bol, N. H. de Leeuw, E. J. M. Hensen and J. P. Hofmann, *ChemSusChem*, 2019, **12**, 4383–4389.

114 P. Thangasamy, S. Oh, S. Nam and I. K. Oh, *Carbon*, 2020, **158**, 216–225.

115 N. Masurkar, N. K. Thangavel and L. M. R. Arava, *ACS Appl. Mater. Interfaces*, 2018, **10**, 27771–27779.

This journal is © The Royal Society of Chemistry 2022

*Energy Environ. Sci.*, 2022, **15**, 1461–1478 | 1477

116 D. Lu, X. Ren, L. Ren, W. Xue, S. Liu, Y. Liu, Q. Chen, X. Qi and J. Zhong, *ACS Appl. Energy Mater.*, 2020, **3**, 3212–3219.

117 S. Maity, B. Das, M. Samanta, B. K. Das, S. Ghosh and K. K. Chattopadhyay, *ACS Appl. Energy Mater.*, 2020, **3**, 5067–5076.

118 J. B. McManus, G. Cunningham, N. McEvoy, C. P. Cullen, F. Gity, M. Schmidt, D. McAteer, D. Mullarkey, I. V. Shvets, P. K. Hurley, T. Hallam and G. S. Duesberg, *ACS Appl. Energy Mater.*, 2019, **2**, 521–530.

119 P. Zhuang, Y. Sun, P. Dong, W. Smith, Z. Sun, Y. Ge, Y. Pei, Z. Cao, P. M. Ajayan, J. Shen and M. Ye, *Adv. Funct. Mater.*, 2019, **29**, 1901290.

120 M. A. R. Anjum, H. Y. Jeong, M. H. Lee, H. S. Shin and J. S. Lee, *Adv. Mater.*, 2018, **30**, 1707105.

121 Q. Zhu, W. Chen, H. Cheng, Z. Lu and H. Pan, *ChemCatChem*, 2019, **11**, 2667–2675.

122 P. A. Le, V. T. Nguyen, V. Q. Le, Y. C. Lu, S. Y. Huang, S. K. Sahoo, Y. H. Chu and K. H. Wei, *ACS Appl. Energy Mater.*, 2021, **4**, 5143–5154.

123 H. Li, J. Zou, S. Xie, X. Leng, D. Gao, H. Yang and X. Mao, *J. Alloys Compd.*, 2017, **725**, 884–890.

124 Z. Liu, N. Li, C. Su, H. Zhao, L. Xu, Z. Yin, J. Li and Y. Du, *Nano Energy*, 2018, **50**, 176–181.

125 X. Guo, J. Ji, Q. Jiang, L. Zhang, Z. Ao, X. Fan, S. Wang, Y. Li, F. Zhang, G. Zhang and W. Peng, *ACS Appl. Mater. Interfaces*, 2017, **9**, 30591–30598.

126 X. Wang, Y. Chen, F. Qi, B. Zheng, J. He, Q. Li, P. Li, W. Zhang and Y. Li, *Electrochem. Commun.*, 2016, **72**, 74–78.

127 Y. Pan, F. Zheng, X. Wang, H. Qin, E. Liu, J. Sha, N. Zhao, P. Zhang and L. Ma, *J. Catal.*, 2020, **382**, 204–211.

128 Y. Sun, X. Zhang, B. Mao and M. Cao, *Chem. Commun.*, 2016, **52**, 14266–14269.

129 J. H. Nam, M. J. Jang, H. Y. Jang, W. Park, X. Wang, S. M. Choi and B. Cho, *J. Energy Chem.*, 2020, **47**, 107–111.

130 Y. Yao, Z. Jin, Y. Chen, Z. Gao, J. Yan, H. Liu, J. Wang, Y. Li and S. (Frank) Liu, *Carbon*, 2018, **129**, 228–235.

131 M. Yang, Z. Sun and Y. H. Hu, *J. Phys. Chem. C*, 2019, **123**, 12142–12148.

132 N. Ling, S. Zheng, Y. Lee, M. Zhao, E. Kim, S. Cho and H. Yang, *APL Mater.*, 2021, **9**, 061108.

133 H. Kim, V. Kanade, M. Kim, K. S. Kim, B. An, H. Seok, H. Yoo, L. E. Chaney, S. Kim, C. Yang, G. Y. Yeom, D. Whang, J. Lee and T. Kim, *Small*, 2020, **16**, 1905000.

134 X. Shang, Y. Rao, S. S. Lu, B. Dong, L. M. Zhang, X. H. Liu, X. Li, Y. R. Liu, Y. M. Chai and C. G. Liu, *Mater. Chem. Phys.*, 2017, **197**, 123–128.

135 J. Li, P. Liu, Y. Qu, T. Liao and B. Xiang, *Int. J. Hydrogen Energy*, 2018, **43**, 2601–2609.

136 S. Balasubramanyam, M. Shirazi, M. A. Bloodgood, L. Wu, M. A. Verheijen, V. Vandalon, W. M. M. Kessels, J. P. Hofmann and A. A. Bol, *Chem. Mater.*, 2019, **31**, 5104–5115.

137 M. Kim, G. H. Park, S. Seo, V. Q. Bui, Y. Cho, Y. Hong, Y. Kawazoe and H. Lee, *ACS Appl. Mater. Interfaces*, 2021, **13**, 11403–11413.

138 J. Li, M. Hong, L. Sun, W. Zhang, H. Shu and H. Chang, *ACS Appl. Mater. Interfaces*, 2018, **10**, 458–467.

139 H. Kwon, B. Ji, D. Bae, J. H. Lee, H. J. Park, D. H. Kim, Y. M. Kim, Y. W. Son, H. Yang and S. Cho, *Appl. Surf. Sci.*, 2020, **515**, 145972.

140 F. Yang, Y. Zhao, Y. Du, Y. Chen, G. Cheng, S. Chen and W. Luo, *Adv. Energy Mater.*, 2018, **8**, 1703489.

141 J. Liu, G. Ding, J. Yu, X. Liu, X. Zhang, J. Guo, J. Zhang, W. Ren and R. Che, *J. Mater. Chem. A*, 2019, **7**, 18072–18080.

142 Y. Zhao, N. Jia, X. R. Wu, F. M. Li, P. Chen, P. J. Jin, S. Yin and Y. Chen, *Appl. Catal., B*, 2020, **270**, 118880.

143 S. Niu, S. Li, J. Hu, Y. Li, Y. Du, X. Han and P. Xu, *Chem. Commun.*, 2019, **55**, 14649–14652.

144 D. Luo, B. Zhou, Z. Li, X. Qin, Y. Wen, D. Shi, Q. Lu, M. Yang, H. Zhou and Y. Liu, *J. Mater. Chem. A*, 2018, **6**, 2311–2317.

145 G. Chen, T. Wang, J. Zhang, P. Liu, H. Sun, X. Zhuang, M. Chen and X. Feng, *Adv. Mater.*, 2018, **30**, 1706279.

146 J. Wang, Z. Wei, S. Mao, H. Li and Y. Wang, *Energy Environ. Sci.*, 2018, **11**, 800–806.

147 S. Anantharaj, P. E. Karthik, B. Subramanian, S. Kundu, S. Balasubramanian and S. Kundu, *ACS Catal.*, 2016, **6**, 4660–4672.

148 Y. Zhang, J. Yan, X. Ren, L. Pang, H. Chen and S. (Frank) Liu, *Int. J. Hydrogen Energy*, 2017, **42**, 5472–5477.

149 S. Anantharaj, K. Karthick, M. Venkatesh, T. V. S. V. Simha, A. S. Salunke, L. Ma, H. Liang and S. Kundu, *Nano Energy*, 2017, **39**, 30–43.

1478 | *Energy Environ. Sci.*, 2022, **15**, 1461–1478

This journal is © The Royal Society of Chemistry 2022